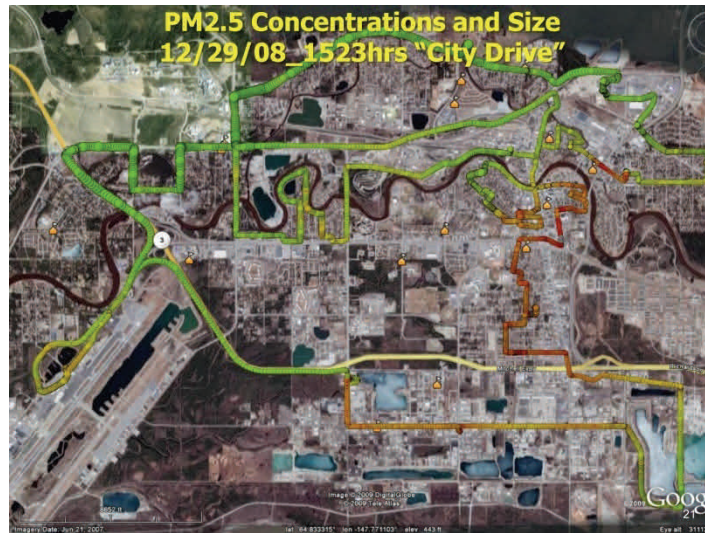# Assessment of the Contribution of Traffic Emissions to the Mobile Vehicle Measured PM$_{2.5}$ Concentration by Means of WRF-CMAQ Simulations

FINAL REPORT
AUTC #410003

Prepared by:

**Prof. Nicole Molders, PhD, PhD
Huy N.Q. Tran, ME**

Date: March 2012

REPORT DOCUMENTATION PAGE	Form approved OMB No.

Public reporting for this collection of information is estimated to average 1 hour per response, including the time for reviewing instructions, searching existing data sources, gathering and maintaining the data needed, and completing and reviewing the collection of information. Send comments regarding this burden estimate or any other aspect of this collection of information, including suggestion for reducing this burden to Washington Headquarters Services, Directorate for Information Operations and Reports, 1215 Jefferson Davis Highway, Suite 1204, Arlington, VA 22202-4302, and to the Office of Management and Budget, Paperwork Reduction Project (0704-1833), Washington, DC 20503

1. AGENCY USE ONLY (LEAVE BLANK)	2. REPORT DATE March 2012	3. REPORT TYPE AND DATES COVERED Final Research Report (8/1/2010-12/31/2011)	
4. TITLE AND SUBTITLE **Assessment of the Contribution of Traffic Emissions to the Mobile Vehicle Measured PM2.5 Concentration by Means of WRF-CMAQ Simulations**		5. FUNDING NUMBERS DTRT06-G-0011 AUTC # 410003	
6. AUTHOR(S) Prof. Nicole Molders, PhD, PhD Huy N.Q. Tran, ME			
7. PERFORMING ORGANIZATION NAME(S) AND ADDRESS(ES) Alaska University Transportation Center University of Alaska Fairbanks P.O. Box 755990 Fairbanks, AK 99775-5900		8. PERFORMING ORGANIZATION REPORT NUMBER INE # 12.05	
9. SPONSORING/MONITORING AGENCY NAME(S) AND ADDRESS(ES) Fairbanks North Star Borough Glen Miller: Director of Transportation P.O. Box 71267 Fairbanks, AK 99707		10. SPONSORING/MONITORING AGENCY REPORT NUMBER	
11. SUPPLENMENTARY NOTES Performed in cooperation with the Fairbanks North Star Borough Air Quality Division.			
12a. DISTRIBUTION / AVAILABILITY STATEMENT		12b. DISTRIBUTION CODE	

13. ABSTRACT (Maximum 200 words)

The Alaska adapted version of the Weather Research and Forecasting and the Community Modeling and Analysis Quality (WRF-CMAQ) modeling systems was used to assess the contribution of traffic to the PM2.5-concentration in the Fairbanks nonattainment area and to develop an algorithm to interpolate mobile measurements into areas without any observations. Simulations were performed with WRF-CMAQ with and without consideration of traffic emission for two episodes in winter 2009/10 and 2010/11.

Comparison of the simulation results with observations showed that the Alaska adapted WRFCMAQ has relatively good performance in simulating meteorological quantities and PM2.5-concentrations. Comparison of the simulations with and without consideration of traffic emissions revealed that emissions from traffic contributed to about 10% on average to the total PM2.5-concentration in the Fairbanks nonattainment area during the two episodes.

The interpolation algorithm was developed based on the WRF-CMAQ results of the first episode and its performance was demonstrated by the results of the second episode. The algorithm can be used in the future to produce spatial distributions of PM2.5-concentrations over the nonattainment area based on the limited observation made by the instrumented vehicle. Theinterpolated distributions can be visualized and put onto the web to serve as a tool to provide spatially differentiated air quality advisory to the public.

14- KEYWORDS : Air quality management, Air quality, National Ambient Air Quality Standards, Pollutants, Exhaust gases, Mobile sources, Geographic information systems, Uncertainty, Simulation, Environmental impacts, Environmental policy, Particulates, Alaska			15. NUMBER OF PAGES 51
			16. PRICE CODE N/A
17. SECURITY CLASSIFICATION OF REPORT Unclassified	18. SECURITY CLASSIFICATION OF THIS PAGE Unclassified	19. SECURITY CLASSIFICATION OF ABSTRACT Unclassified	20. LIMITATION OF ABSTRACT N/A

Table of Contents

List of Figures

Fig. 1. Mobile platform and its outside measurement equipment. The 2007 FNSB-owned Ford Explorer is equipped among other things with a data RAM4000 monitor, BGi $PM_{2.5}$ sharp cut cyclone, sample liner heaters, Garmin GPS, DryCal flow calibrator, temperature loggers, and a 300W power converter.

Fig. 2. $PM_{2.5}$-concentrations as measured in Fairbanks by the sniffer (lines of dots) on 12-29-2008 during the drive starting at 1523 AST. Measurements have been also made in the hills and the North Pole area (not shown here). Single dots are the stationary sites. Color code: deep green 0-35$\mu g/m^3$, olive 35-105$\mu g/m^3$, orange 105-210$\mu g/m^3$, red 210-350 $\mu g/m^3$, and >350 $\mu g/m^3$ grey.

Fig. 3. Schematic view of the simulation domain. The CMAQ simulations are performed on domain D3 only. The WRF simulations on domain 1 (entire area) and domain 2 (D2) served to downscale the NCEP final analysis data.

Fig. 4. Schematic view of the CMAQ modeling package [from *CMAQ v.4.7.1 Operational Guidance Document*; 2010]. In our simulations, WRF serves as the meteorology modeling system, and the Sparse Matrix Operator Kernel Emissions (SMOKE; [*Houyoux et al., 2007*]) version 2.6 serves as the emission modeling system.

Fig. 5. 24-hour average $PM_{2.5}$-concentrations as measured at the fixed monitoring sites in Fairbanks nonattainment area from (top) 11/01/2009 to 02/28/2010 and (bottom) 11/01/2010 to 02/28/2011. Here, SB is the site at the State Office Building; PR is the site located at the Transit Administration Center on Peger Road, RAMS stands for Relocatable Air Monitoring System, NP is the site located at the North Pole Elementary School and NCORE is the site located at Pioneer Road. Note that the RAMS was relocated several times each winter.

Fig. 6: Temporal evolution of daily averaged air-temperatures T (^{o}C), wind-speed v (m/s), relative humidity RH (%), daily accumulated downward shortwave radiation SW (W/m^2), and sea-level pressure SLP (hPa) averaged over the 14 observational sites for which data was available in episode 1. Solid blue line and closed circles indicate simulated and observed quantities; grey-shading and vertical bars indicate the variance of the simulated and observed quantities, respectively.

Fig. 7: Like Fig. 6, but for all 18 observational sites for which data was available in episode 2.

Fig 8: Temporal evolution of simulated and observed (left) hourly and (right) 24h-average $PM_{2.5}$-concentrations as obtained at the SB site for episode 1 (upper part) and 2 (lower part). Dashed blue and solid black lines indicate simulated and observed quantities, respectively.

Fig 9: Scatter (left) and soccer (right) plots of simulated and observed 24h-average $PM_{2.5}$-concentrations at the monitoring sites for which data was available during episode 2. The black, green and blue lines in the scatter plots indicate the 1:1-line and a factor of two and three agreement between pairs of simulated and observed values, respectively.

Fig. 10. Scatter plots (upper part) and population distribution plots (lower part) of simulated temperatures and $PM_{2.5}$-concentrations vs. temperatures and $PM_{2.5}$-concentrations measured by the sniffer for all sniffer drives during episode 1.

Fig. 11. Like Fig. 10, but for all sniffer drives during episode 2.

Fig. 12. Average PM$_{2.5}$-emission in (a) REF and zoom-in on (b) PM$_{2.5}$-emission differences (REF-NTE) for episode 1. The red polygon indicates the Fairbanks PM$_{2.5}$-nonattainment area. Similar emission patterns were found for episode 2 (not shown).

Fig. 13. Zoom-in on the average PM$_{2.5}$-differences REF-NTE (left) and the average RRF (NTE/REF) for episode 1 with wind barbs overlaid. The nonattainment area, grid-cell holding the official monitoring site at the State Office Building and grid-cells traveled by instrument vehicle are represented by the blue polygon, blue star and white dots, respectively. North Pole (NP), Fort Wainwright (FT) and hills (HL) regions are represented by cyan, purple and white polygons, respectively, and the remaining region is Fairbanks City (FC). Downtown area (DT) is indicated by the black square. Note that these lines are not the administrative boundaries.

Fig. 14. Like Fig. 13, but for episode 2.

Fig 15: Highest 24h-average PM$_{2.5}$-concentrations in REF (blue line) and in NTE (green line), and highest 24h-average PM$_{2.5}$-difference (dash red line) as obtained (left) on average over the nonattainment area and (right) at the SB site in episode 1.

Fig 16: Like Fig. 15, but for episode 2.

Fig. 17. Interpolated (ITP) vs. simulated, i.e. "grand truth" (SIM) as obtained with the algorithm using the WRF-CMAQ data for 01/11/2011 as "proxy" for observation in the nonattainment area. The black triangle indicates the grid-cells covered with the assumed sniffer route on this day.

Fig. 18. Like Fig. 17, but for 01/18/2011

Fig. 19. Overall performance of the recommended interpolation algorithm (without consideration of wind direction) as obtained for episode 2.

Fig. 20. Like Fig. 19, but for the interpolation algorithm with consideration of wind direction.

Fig. 21. Like Fig. 19, but for the 100 random samples.

Fig. 22. Recommended sniffer route.

Fig. 23. Like Fig. 19, but for the recommended route.

Fig. 24. Diagram of the data flow to obtain interpolated PM$_{2.5}$-concentration distributions from mobile measurements.

List of Tables

Acknowledgements

Abstract

The Alaska adapted version of the Weather Research and Forecasting and the Community Modeling and Analysis Quality (WRF-CMAQ) modeling systems was used to assess the contribution of traffic to the $PM_{2.5}$-concentration in the Fairbanks nonattainment area and to develop an algorithm to interpolate mobile measurements into areas without any observations. Simulations were performed with WRF-CMAQ with and without consideration of traffic emission for two episodes in winter 2009/10 and 2010/11.

Comparison of the simulation results with observations showed that the Alaska adapted WRF-CMAQ has relatively good performance in simulating meteorological quantities and $PM_{2.5}$-concentrations. Comparison of the simulations with and without consideration of traffic emissions revealed that emissions from traffic contributed to about 10% on average to the total $PM_{2.5}$-concentration in the Fairbanks nonattainment area during the two episodes.

The interpolation algorithm was developed based on the WRF-CMAQ results of the first episode and its performance was demonstrated by the results of the second episode. The algorithm can be used in the future to produce spatial distributions of $PM_{2.5}$-concentrations over the nonattainment area based on the limited observation made by the instrumented vehicle. The interpolated distributions can be visualized and put onto the web to serve as a tool to provide spatially differentiated air quality advisory to the public.

Summary of Findings

1. The Alaska adapted version of WRF-CMAQ has acceptable performance in simulating meteorological and $PM_{2.5}$-concentration in the Fairbanks nonattainment area for the two episodes of our study. This means it is suitable as the reference WRF-CMAQ model setup for future model studies on air quality in Fairbanks and its neighborhood.

2. WRF-CMAQ simulations performed with and without traffic emission revealed contribution of traffic emission to the total $PM_{2.5}$-concentration in the Fairbanks nonattainment area is about 10% on average in both episodes. In the nonattainment area, traffic contributions vary in space with the highest contributions in the downtown area and the lowest in the hills (Goldstream Valley).

3. An algorithm to interpolate $PM_{2.5}$ measured by the mobile instrumented platforms into areas without measurements was developed for the Fairbanks nonattainment area. The accuracy of the interpolation algorithm heavy depends on the area covered by the mobile platforms at the time of interpolation. Assessment of the developed interpolation algorithm revealed an overall correlation between interpolated and simulated $PM_{2.5}$-concentrations >0.720, normalized mean biases between -30 and 60%, and normalized mean errors <100%.

4. A mobile platform travel route that yielded best interpolation accuracy is recommended. The algorithm makes use of the gradients and ratios of concentrations found for various neighborhoods. Note that the algorithm can be transferred to other urban areas with mobile measurements, but in that case needs WRF-CMAQ simulations for that urban area.

CHAPTER 1 - INTRODUCTION AND RESEARCH APPROACH

1.1 Problem Statement and Research Objective

Recently, the Environmental Protection Agency (EPA) lowered the 24-hour National Ambient Air Quality standard (NAAQS) for particulate matter (PM) with aerodynamic diameter $< 2.5\mu m$ (PM$_{2.5}$) to $35\mu g/m^3$. Since observational data indicated that PM$_{2.5}$ concentrations exceeded the new standard periodically during the past years [e.g. *Tran and Mölders*, 2011], Fairbanks was assigned a PM$_{2.5}$-nonattainment area. To develop strategies to achieve and retain compliance, a State Implementation Plan (SIP) has to be developed.

Fig. 1. Mobile platform and its outside measurement equipment. The 2007 FNSB-owned Ford Explorer is equipped among other things with a data RAM4000 monitor, BGi PM$_{2.5}$ sharp cut cyclone, sample liner heaters, Garmin GPS, DryCal flow calibrator, temperature loggers, and a 300W power converter. Courtesy to *F. di Genova* [2009]

To be able to prepare a SIP, various actions were taken. The Fairbanks North Star Borough (FNSB) expanded their stationary monitoring network (Sadler's, Nordale School, Peger Road, North Pole, moveable trailer) since winter 2008/09. At the stationary sites, PM$_{2.5}$, sulfur oxide (SO$_x$), nitrogen oxide (NO$_x$=NO+NO$_2$), black carbon, temperature, wind speed and direction were collected. The FNSB also instrumented vehicles (Fig. 1) - called sniffer hereafter - to collect PM$_{2.5}$-concentration data downtown, in North Pole, and the hills to obtain a broad picture of the PM$_{2.5}$-concentration distribution within the nonattainment area.

The FNSB has taken sniffer measurements of PM$_{2.5}$-concentrations using instrumented vehicles since winter 2008/09. For example, from November 2008 to February 2009, the mobile platforms collected 370h of GPS-positioned data of PM$_{2.5}$ including speciation and temperature (e.g. Fig. 2). In 2008/09, 664,000 data records (1 every 2 seconds) were taken. Seventeen drives were performed on days with exceedances of the NAAQS.

The mobile measurements are instantaneous values collected by a moving sampler traveling at 20-35miles/hour. It takes about 1h or more to cover the "measurement routes" of the nonattainment area. Based on the sniffer measurements and the data from the stationary sites, the following rough picture of the spatial distribution and temporal variations exists [*Conner*, 2009 pers. com.]. The PM$_{2.5}$-concentrations recorded along Airport Way and the Mitchell Highway in and around North Pole are relatively high, extremely low east of North Pole in the flood plain, increased in the vicinity of Moose Creek and lower again towards Eielson Air Force Base. The mobile data also showed a buildup in concentration during the

day with a peak at 1800 Alaska Standard Time (AST) and a secondary peak at 2400 AST. In the most densely populated areas, concentrations were highest between 1600 and 1800 AST.
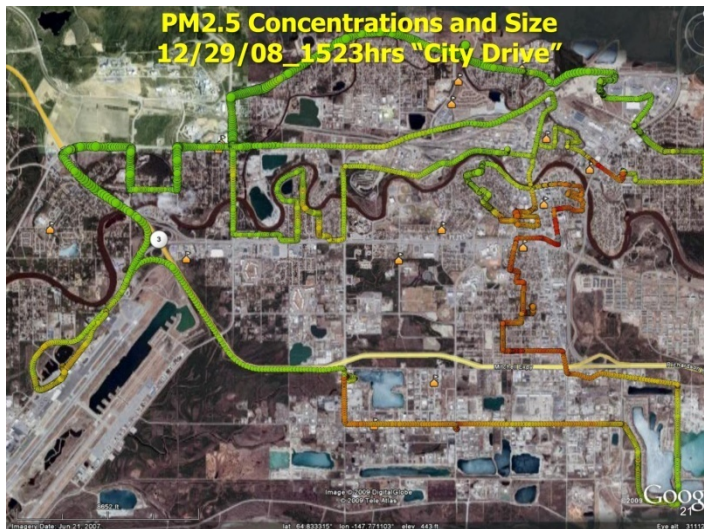
Fig. 2. $PM_{2.5}$-concentrations as measured in Fairbanks by the sniffer (lines of dots) on 12-29-2008 during the drive starting at 1523 AST. Measurements have been also made in the hills and the North Pole area (not shown here). Single dots are the stationary sites. Color code: deep green 0-35μg/m^3, olive 35-105μg/m^3, orange 105-210μg/m^3, red 210-350μg/m^3, and >350μg/m^3 grey. Courtesy to *F. di Genova* [2009]

The FNSB found it desirable to interpolate the mobile and stationary measurements into areas without data. However, they were concerned doing so without knowledge about the temporal and spatial scaling issues as there are various emission sources in the neighborhoods that might affect the $PM_{2.5}$-concentrations. Such knowledge is needed to interpolate monitored concentrations into or assess the impact of planned roads on air quality in neighborhoods adjacent to major traffic lines. One goal of our study was to develop an interpolation algorithm that would address these issues and permit a knowledgeable interpolation. The idea was that this interpolation algorithm could serve as a tool to provide spatial distributions of $PM_{2.5}$-concentrations for public air quality advice. The public had frequently approached the FNSB that the FNSB should provide a regionally differentiated air quality advisory.

Since traffic is one of the potential sources and contributors to $PM_{2.5}$-concentrations, another goal of this study was to assess the contribution of traffic to the $PM_{2.5}$-concentrations at breathing level. Thus, our research included assessing the traffic-emission impacts on observed concentrations under various traffic as well as cold weather conditions using an Alaska-adapted version of EPA's regulatory model called WRF-CMAQ [*Mölders and Leelasakultum* 2011].

1.2 Scope of Study

We used the Alaska adapted version of the WRF-CMAQ model [*Mölders and Leelasakultum* 2011]. The WRF-CMAQ simulations were performed with and without inclusion of traffic emissions, while all other emissions were kept the same. Simulations were performed for two episodes in winter 2009/10 and 2010/11 that had days with mobile measurements. The results of the simulations with consideration of traffic emissions performed for the first episode served to develop the interpolation algorithm. The results of the simulations with consideration of traffic emissions preformed for the second episode served to test the interpolation algorithm and assess its accuracy. Simulation results of both

3

episodes were used to assess the impact of traffic emissions on Fairbanks' $PM_{2.5}$-situation. The work also intended to help assess emission control measures to mitigate Fairbanks' $PM_{2.5}$ problem.

The results of these simulations with and without consideration of traffic emissions were compared to each other to assess the contribution of traffic emissions to the $PM_{2.5}$ concentrations in the nonattainment area. Ratios of concentrations from the simulations with and without consideration of traffic provide the fractional contribution of traffic to the concentrations and the relative response factor (RRF).

The scopes of the proposed research were to:

- Evaluate the performance of WRF-CMAQ with respect to simulating $PM_{2.5}$-concentrations;
- Determine the contribution of traffic emissions to the $PM_{2.5}$-concentrations in the nonattainment area for selected episodes in winter 2009/10 and/or 2010/11 by means of WRF-CMAQ results from simulations with and without consideration of traffic emissions to better assess potential means for improving air quality during the winter months. Ratios of the simulated concentrations with consideration of traffic emissions to those obtained without consideration of traffic emissions provide the fractional contribution of traffic to the concentration at each model grid cell. The goal was to assess the percentage contribution in space and time;
- Provide interpolation algorithms for interpolating sniffer's measurements to areas where measurements are not applicable. The method of interpolation can be used in cooperated with GIS applications to interpolate future sniffer's measurements onto maps of concentration distribution in the Fairbanks nonattainment area;
- Assess the degree of uncertainty, and assess the differences between the highly complex research model WRF/Chem [*Peckham et al.,* 2009; *Mölders et al.*, 2011a; 2012] and the less complex WRF-CMAQ package by comparison of their results.

1.3 Research Approach

This research applied numerical modeling techniques to assess the contribution of traffic emissions to Fairbanks' $PM_{2.5}$ problem. The technical question we addressed is how to simply, but reasonably interpolate mobile measurements into space without the need to run an air-quality forecast (AQF) model.

For regulatory and permitting purposes, EPA typically uses the WRF plus the Community Multiscale Air Quality (CMAQ; *CMAQ v.4.7.1 Operational Guidance Document* [2010]) modeling structure (called WRF-CMAQ hereafter). Therefore, we used the WRF-CMAQ as our main modeling tool. However, as bottom-up emission inventory became available much later than anticipated, we also used WRF/Chem to assess traffic impacts for October 2008 to March 2009. We also used WRF/Chem simulations to develop the method to project mobile measurements onto a model domain and to develop and test the quality assurance and quality control (QA/QC) for the mobile measurements [*Mölders et al.*, 2012].

1.3.1 Simulation Setup

The meteorology quantities were simulated by WRF version 3.1 in the physical setup suggested by *Gaudet and Stauffer* [2010] for the Fairbanks SIP development. This means the

simulations were run in a two-way nesting mode with three domains. The outermost and largest domain (domain 1) encompasses Alaska, and parts of Siberia, the North Pacific and Arctic Ocean with 400×300grid-cells of 12km increment (Fig. 3). Domain 2 covers central Alaska with 201×201grid-cells of 4km increment. The inner most domain encompasses the nonattainment area and the western part of the FNSB with 201×201grid-cells of 1.3km increment (Fig. 3). In this configuration, simulations were performed concurrently in all 3 domains with boundary conditions for in inner domain were taken from simulation of its mother domain. In contrast to *Gaudet and Stauffer* [2010], we did not use data assimilation, as data assimilation may be problematic when the number of radiosonde soundings is low, when only IR satellite imagery is available like it is the case in winter in Alaska or when the resolution is very high (i.e. the grid-increments are very small). At high resolution, data assimilation may smooth out inversions that locally build in valleys. Radiosondes typically do not report before they have reached a height of a couple of decameter. However, in Fairbanks, inversions often occur below such heights. Thus, assimilation to radiosonde derived temperature and/or wind data may bear the risk that the assimilation might smooth out inversions that developed (correctly) in the model.

The CMAQ simulations were performed on domain 3 only. Alaska typical background concentrations served as initial and boundary conditions for the chemical fields. Note that investigations by *Cahill* [2003], *Tran et al.* [2011] and *Mölders et al.* [2012] showed that hardly any $PM_{2.5}$ in notable concentrations ($>2\mu g/m^3$) is advected into the area covered by domain 3.
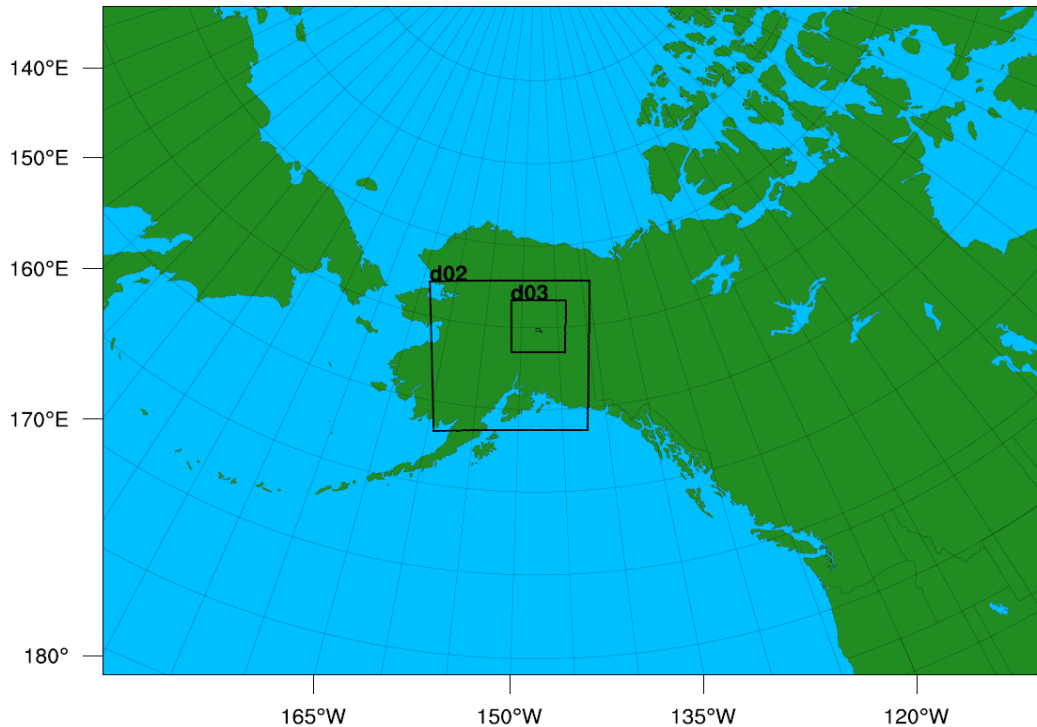

Fig. 3 Schematic view of the simulation domain. The CMAQ simulations are performed on domain D3 only. The WRF simulations on domain 1 (entire area) and domain 2 (D2) served to downscale the NCEP final analysis data.

The selections of the physical option for the WRF simulation were based on the experience from previous studies with WRF are those recommended by *Gaudet and Stauffer* [2010] (Table 1). Note that *Mölders and Kramm* [2007] used a similar set up. *Mölders and Kramm* [2010] tested various setups and recommended a similar setup.

Meteorology initial conditions were re-initialized for every 5 days. The WRF domain 1 was initialized with the National Centers for Environmental Prediction (NCEP) Final Analysis (FNL) data that were produced with the Global Forecast System (GFS). The FNL data have a $1^{o} \times 1^{o}$ spatial resolution and a 6h temporal resolution. This data also serves as lateral boundary conditions to the WRF on domain 1. The initial conditions of domain 2 and 3 are provided by the respective parent domain. Domains 2 and 3 exchange data in both directions (two-way nesting). This means that what goes on in domain 3 affects domain 2 and vice versa. The same applies to domains 1, and 2. Since we did no data assimilation, we re-initialized WRF every 5 days.

The chemical fields in CMAQ were initialized with the background concentration profiles of the Alaska adapted CMAQ described in *Mölders and Leelasakultum* [2012]. Since CMAQ needs some time to spin up the chemical fields, the chemical fields at the end of a simulation served as the initial conditions for the next simulation. This means only the simulation for the first day used the Alaska typical background concentrations as initial condition, and that this procedure avoids having to discard model results for spin-up every 5 days. We examined the spin up time for each episode separately and discarded the data of the spin up time.

Table 1. Parameterizations used in the WRF simulations.

Processes	Scheme and reference
Cloud microphysics	Six water-class cloud microphysical scheme [*Hong and Lim*, 2006]
Subgrid-scale convection	Improved 3D-version of the Grell-Dévényi cumulus-ensemble scheme [*Grell and Dévényi*, 2002]
Radiation	Goddard shortwave radiation scheme [*Chou and Suarez*, 1994], Radiative Transfer Model for long-wave radiation [*Mlawer et al.*, 1997], Radiative feedback from aerosols [*Barnard et al.*, 2010]
Atmospheric boundary layer and sublayer processes	Mellor-Yamada-Janjić scheme [Janjić, 1994]
Land-surface processes	Modified version of the Rapid Update Cycle land-surface model [*Smirnova et al.*, 2000]

The chemical and aerosol processes transport, diffusion and removal of species were simulated by CMAQ version 4.7 for the finest resolved domain (i.e. domain 3) which extends 199×199grid-cells with 1.3km increment and covers Fairbanks and its neighborhoods (Fig. 3). This domain is one grid-cell less to each side of the WRF domain 3 due to the fact that those outmost grid-cells serve as boundaries for the CMAQ domain. The domain has 38 full vertical layers, and is centered at 64.92749N and 147.957W.

Originally, we had planned to perform the WRF-CMAQ simulations on a smaller domain with about 444m grid-increment. However, we had to abandon this plan as the bottom-up

emission inventory did not become available with this resolution and we had to start the development of the algorithm. As the 444m resolution bottom-up emission inventory for Fairbanks did not become available, we could not create emissions at this resolution and hence not perform simulations at this resolution as well.

We applied the CMAQ's modifications and optimized settings for Alaska conditions that had been recommended by *Mölders and Leelasakultum* [2011]. Those modifications and optimized settings include: modifications of dry deposition mechanism to consider deposition on Alaska's land cover types including snow following *Mölders et al.* [2011a] and tundra; modification of the minimum mixing height from 50m to 16m as observed in Fairbanks [*Wendler* 2008; pers. comm.]; application of Alaska's chemical background concentrations as initial and boundary concentrations in CMAQ [*Mölders and Leelasakultum*, 2011]; selection of global-mass-conserving scheme (YAMO) as advection scheme; modification of eddy diffusivity coefficients (Kz_min, KZL, KZU); and choice of inline-calculation of photolysis rates[*Mölders and Leelasakultum*, 2011].

We performed simulations with (REF) and without consideration of traffic emission (NTE). In NTE, all emissions from on-road vehicles were excluded, while keeping all other emissions the same as in REF.
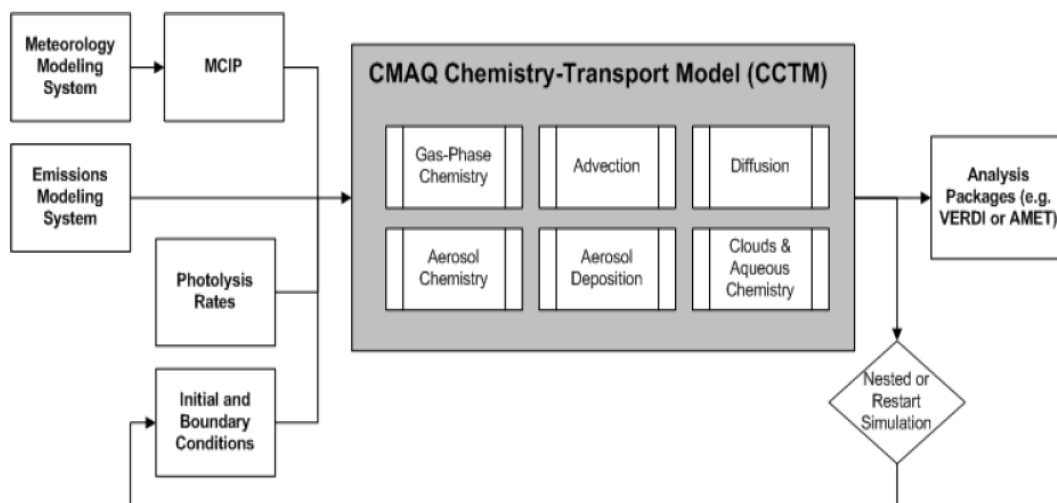
Fig. 4. Schematic view of the CMAQ modeling package. From *CMAQ v.4.7.1 Operational Guidance Document* [2010]. In our simulations, WRF serves as the meteorology modeling system, and the Sparse Matrix Operator Kernel Emissions (SMOKE; *Houyoux et al.* [2007]) version 2.6 serves as the emission modeling system.

1.3.2 Selection of the Simulation Episodes

The simulation episodes were selected to represent days having NAAQS exceedance events detected at the State Office Building (SB) site (the official monitoring site) and concurrently having high $PM_{2.5}$-concentrations at numerous locations detected by the sniffer measurement.
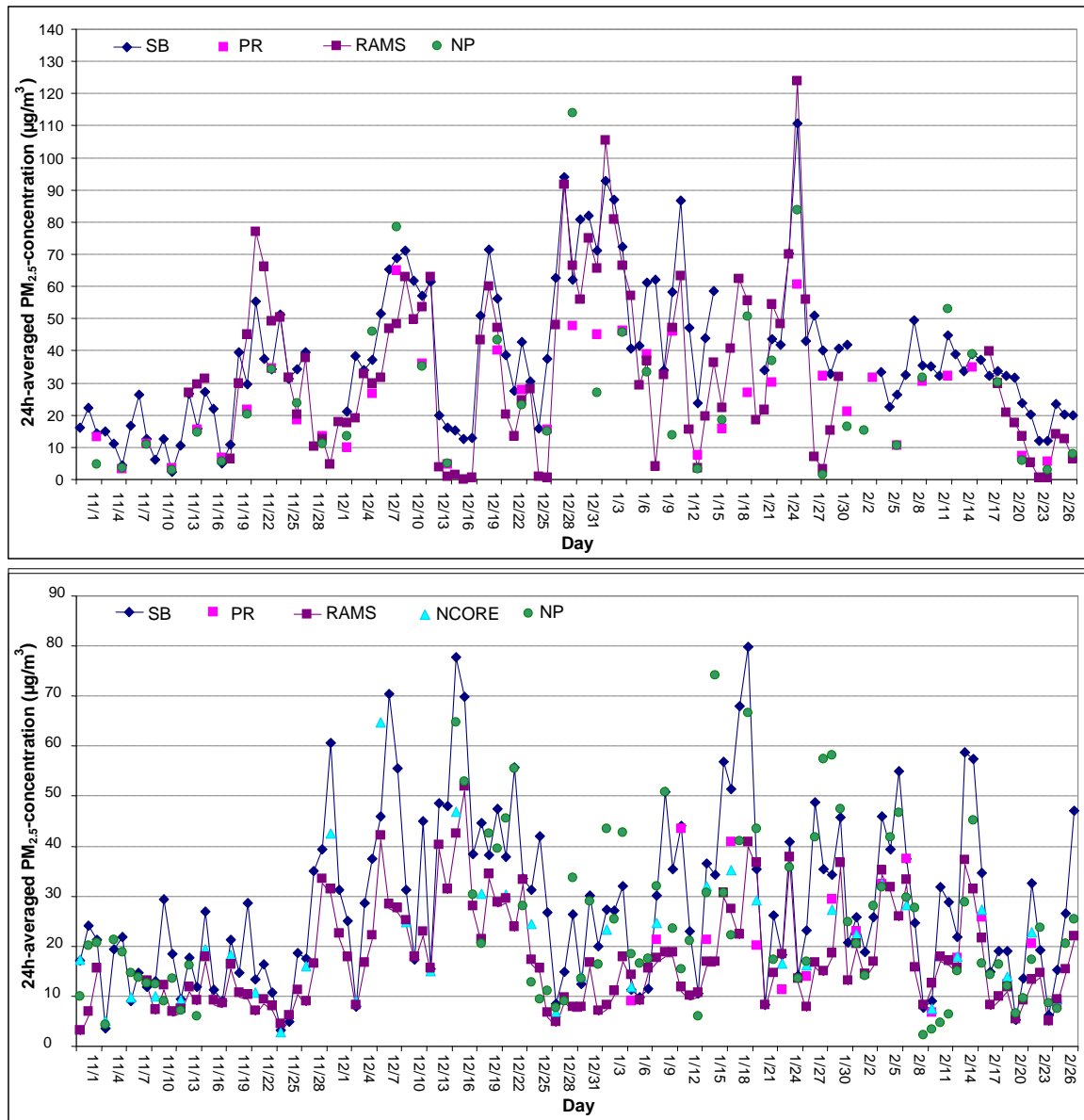
Fig. 5. 24-hour average PM$_{2.5}$-concentrations as measured at the fixed monitoring sites in Fairbanks nonattainment area from 11/01/2009 to 02/28/2010 (upper panel) and 11/01/2010 to 02/28/2011 (lower panel). Here, SB is the site at the State Office Building; PR is the site located at the Transit Administration Center on Peger Road, RAMS stands for Relocatable Air Monitoring System, NP is the site located at the North Pole Elementary School and NCORE is the site located at Pioneer Road. Note that the RAMS was relocated several times each winter.

During November 1 2008 to February 28 2009, several periods of exceedance days were observed at the State Office Building site (Fig. 5). On January 26 2009, the day with the highest exceedance, the 24h-average PM$_{2.5}$-concentration was 110μg/m^3. This event was within a period of a few days that had daily exceedances, however, only a limited amount of mobile measurements. Therefore, we decided to use the period from December 27 2009 to January 11 2010 as the training episode for the development of the interpolation algorithm.

During this episode, there were 14 days that continuously exceeded the NAAQS, and many mobile measurements were made, and high $PM_{2.5}$-concentration were also observed by the sniffer. The simulation was started three days earlier (December 24 2009) to spin up the model. Note that the spin-up data were not considered in the analysis, evaluation or development of the interpolation algorithm.

In winter 2010/11, the observations showed high $PM_{2.5}$-concentrations that exceeded the NAAQS at various stationary sites from December 2010 through February 2011. There were more exceedances in December than in January and February (Fig. 5). However, there were much fewer sniffer drives in winter 2010/11 than in winter 2009/10, and no drive was performed during December 2010. We decided to choose January 1-21 2011 as the second simulation episode 2 that would serve for assessment of the interpolation algorithm. Note that during that episode seven sniffer drives were performed.

The simulation data from both episodes were used to assess the contribution of traffic to the $PM_{2.5}$-concentrations at breathing level.

For the development and testing of the method to project the mobile measurements onto a model domain, we used WRF/Chem simulations that covered October 1, 2008 to April 1, 2009. Note that these WRF/Chem simulations used the National Emission Inventory 2008 and the Alaska Emission allocation Model [*Mölders* 2010], i.e. a top-down emission inventory. Differences between bottom-up and top-down emission inventories are widely discussed in the literature and therefore not repeated here. See, for instance, *Mölders et al.* [2011a] for a brief discussion.

1.3.3 Emission Inventory

Anthropogenic emissions for the WRF-CMAQ simulations were based on the Fairbanks' emission inventory in 2008 (draft version) developed by Sierra Research Inc.. To apply this emission inventory of 2008 to the simulation year (i.e. winter 2009/2010 and winter 2010/2011), we assumed that the emissions increased by 1.5%/year in accord with *Mölders* [2011a; 2012]. This "updated" emission inventory was allocated onto the CMAQ domain in time and space by SMOKE based on the emission sources' activities, and the land-use and population density within each grid-cell.

Anthropogenic emissions include emission from point sources, area sources (e.g. domestic and commercial heating, industry, power plants, etc.), traffic and non-traffic (snow mobiles, railroad, etc.). Biogenic emissions were excluded from the simulations as no data was available. However, the WRF/Chem simulations showed that we can consider biogenic emissions as marginal during winter in Fairbanks itself.

We applied a temperature adjustment factor to the temporal allocation of the anthropogenic emission. In this approach, the emission will be higher (lower) in day having temperature lower (higher) than the monthly mean temperature as described in *Mölders* [2010] and *Mölders et al.* [2011a, b; 2012].

The treatment of the emission data used for WRF/Chem is described in *Mölders* [2010] and *Mölders et al.* [2011a, b; 2012].

1.3.4 Analysis Methods

We calculated performance skill–scores following *von Storch* and *Zwiers* (1999) to evaluate the WRF-CMAQ performance with respect to simulating meteorological quantities. These skill scores include the bias, root–mean–square error (RMSE), standard deviation of error (SDE), and the correlation skill score (R). Note that this score is identical to a correlation coefficient.

We evaluated the simulated $PM_{2.5}$-concentrations in accord with *Boylan* and *Russell* [2006]. In doing so we determined the fractional bias $\left(FB = \left[\frac{2}{N}\sum_{i=1}^{N}\frac{(C_{s,i}-C_{o,i})}{(C_{s,i}+C_{o,i})}\right]\cdot 100\%\right)$, fractional error $\left(FE = \left[\frac{2}{N}\sum_{i=1}^{N}|C_{s,i}-C_{o,i}|/(C_{s,i}+C_{o,i})\right]\cdot 100\%\right)$, normalized mean bias $\left(NMB = \left[\sum_{i=1}^{N}(C_{s,i}-C_{o,i})/\sum_{i=1}^{N}C_{o,i}\right]\cdot 100\%\right)$, normalized means error $\left(NME = \left[\sum_{i=1}^{N}|C_{s,i}-C_{o,i}|/\sum_{i=1}^{N}C_{o,i}\right]\cdot 100\%\right)$, and the performance goals and criteria. In addition we determined the fraction of pairs of simulated (C_s) and observed (C_o) $PM_{2.5}$-concentrations that agreed within a factor of two (FAC2). The correlation R between measured and observed quantities was tested for their statistical significant using the Student t–tests at the 95% confidence level.

As the FNSB was interested in whether traffic is a main contributor to exceedances, we examined how many "exceedances" and "exceedance-days" were avoided in the simulations without consideration of traffic emissions as compared to the simulations that considered all emissions. In doing so, we considered 24h-average $PM_{2.5}$-concentrations being greater than the NAAQS at any grid-cell on any day as an "exceedance", and any day that had at least one "exceedance" anywhere in the nonattainment area as an "exceedance-day".

We calculated the relative response factors (RRF) to assess the effects of traffic emissions over the nonattainment area. The RRF is the ratio of the concentration in the simulation without traffic to the concentration in the simulation with traffic. Thus, we divided the 24h-average $PM_{2.5}$-concentration obtained by the simulation without considerations of traffic emissions by those obtained by the simulations that considered all emissions. The RRFs were calculated for all grid-cells in the nonattainment area including the grid-cell that holds the official monitoring site at the State Office Building. Subtraction of the RRF from 1 provides the percentage reduction. Multiplication with the design value permits to assess what design value would be observed if there was no traffic. However, assessing the design value for a Fairbanks without traffic emission was beyond the scope of this study and therefore was not performed and is not discussed.

1.3.5 $PM_{2.5}$ Interpolation Algorithm

In the interpolation algorithm, each grid-cell in the nonattainment area is to be interpolated from grid-cells that have sniffer measurements. Recall that a grid-cell extends 1.3km×1.3km. To develop the interpolation algorithm we used WRF-CMAQ to provide a test dataset. We used the WRF-CMAQ simulated $PM_{2.5}$-concentrations as the "grand truth", i.e. the WRF-CMAQ data are assumed to represent the actual situation on a given day. The concentrations in the grid-cells that on a given day were assumed to be traveled by the sniffer were pulled as the "observed sniffer data". We developed an interpolation algorithm that is a linear-regression of the $PM_{2.5}$-concentration at the grid-cell for which a concentration has to be

interpolated with the PM$_{2.5}$-concentration at the grid-cells traveled by the sniffer. The development of the linear-regression interpolation procedure worked as follows:

1. We performed a quality assurance/quality control (QA/QC) on all mobile measurements following *Mölders et al.* [2012]. This QA/QC discarded all temperature and PM$_{2.5}$-data for which the measured temperature deviated more than the 1971-2000 monthly-mean diurnal temperature range from the mean temperature determined from all temperature-data of the respective drive. Note that at the time of this work the 1981-2010 temperature average were not yet available. This QA/QC ensured to discard data taken when the vehicle pulled out and the sensors were still adjusting to the outside air. The QA/QC-procedure also discarded all PM$_{2.5}$-concentrations that differed >5μg/m^3 between two consecutive measurements to avoid errors from plumes from buses or trucks that emit at about the sniffer height (~2.44m) and may have hit the sniffer.

2. In accord with *Mölders et al.* [2012], we projected the remaining data onto the model-grid and averaged over all measurements that were taken in the same grid-cell and hour. These concentrations provide data for some of the grid-cells in the nonattainment area, namely those where the measurements were made.

3. To develop the interpolation algorithm, we identified various route like they are usually driven by the FNSB with the instrumented vehicles. For the grid-cells on these routes we pulled the simulated PM$_{2.5}$-concentrations from the WRF-CMAQ data. Using the simulated concentrations at these grid-cells we constructed linear-regression equations for all other grid-cells in the nonattainment area, i.e. all grid-cells that are not on the assumed route. This means that for different routes, we developed different sets of linear-regression equations. These equations will later serve to describe the relationship of the measured PM$_{2.5}$-concentration along the respective route and the grid-cells in the nonattainment area for which no measurements were made during a drive. The linear-regression equations look as follows

$$C_{i\,(itp)} = \sum_j^n a_j C_{j\,(obs)} + b \qquad\qquad (1)$$

where $C_{i(itp)}$ is the interpolated concentration at the grid-cell i for which a value has to be determined, $C_{j(obs)}$ is the concentration at the grid-cell j where a measurement was made. Furthermore, n is the total number of grid-cells that were covered by the drive, and a_j and b are the linear-regression coefficients, respectively.

To develop the above equations we used simulated concentrations instead of observed concentrations. Doing so is necessary as there was no special field campaign that took measurements in each of the grid-cells of the nonattainment area that we could have used to test and develop the algorithm. In the development, we used the simulated concentrations that were not on an assumed route as the goal of concentrations that our interpolation algorithms should provide. During the development, we evaluated the accuracy of the interpolation algorithm by comparing the WRF-CMAQ simulated

concentrations with the concentrations that were provided by the interpolation algorithm based on the WRF-CMAQ concentrations along the assumed route.

At the start of the development of the algorithm, we considered the concentrations at all grid-cells on the assumed route. To optimize the accuracy of the above equations, we determined the adjusted determination coefficient

$$R^2_{adj} = 1 - \frac{\sum_l^m (C_{i(itp),l} - C_{i(sim),l})^2 (m-1)}{\sum_i^m (C_{i(sim),l} - \overline{C_{i(sim)}})^2 (m-n-1)} \tag{2}$$

where $C_{i(sim)}$ and $\overline{C_{i(sim)}} = \frac{1}{m}\sum_l^m C_{i(sim),l}$ are the simulated and the mean of the simulated concentrations at the grid-cells without assumed measurements. Furthermore, m is the size of the sample (i.e. the total number of hours of simulated data used to develop Eq. (1)).

As suggested by Eq. (2), the closer R^2_{adj} is to 1, the lower is the error of the interpolation. The value of R^2_{adj} only increases, when the concentrations $C_{j(sim)}$ in the grid-cells of the assumed route are important to describe the concentration $C_{i(itp)}$ at the grid-cell i. The letter i denotes the grid-cell for which the interpolation is to be done. The value of R^2_{adj} decreases when a concentration $C_{j(sim)}$ at a grid-cell of the assumed route is unimportant to determine $C_{i(itp)}$. This means that not all concentrations along the assumed route are needed for the determination of the concentration at a grid-cell outside the assumed route. Note that usually only grid-cells in the vicinity of grid-cell i are finally considered in Eq. (1).

To determine which of the grid-cells along the assumed route are to be excluded from Eq. (1), we calculated the standardized regression coefficient A_j. This coefficient indicates the importance of the concentration $C_{j(sim)}$ at the grid-cell j on the assumed route for the concentration at the grid-cell i outside the route, i.e. the interpolated concentration $C_{i(itp)}$

$$A_j = a_j \frac{standard\ deviation\ of\ C_{j(sim)}}{standard\ deviation\ of\ C_{i(itp)}} \tag{3}$$

The concentration $C_{j(sim)}$ at a grid-cell j of the assumed route for which A_j is the lowest was excluded. Then Eq. (1) was reformulated with the concentrations $C_{j(sim)}$ at the remaining grid-cells $j=1,..., N$ of the assumed route. Here N is the number of remaining grid-cells on the assumed route. The procedure was repeated until the obtained R^2_{adj} reached a maximum.

For a given assumed route we have as many interpolation equations as there are grid-cells for which a value has to be interpolated. Or in other words, we have k-n equations where k is the total number of grid-cells in the nonattainment area and n is the number of grid-cells on the route.

Note that Eq. (1) was developed based on the routes that the sniffer made measurement on during episode 1. This means there is no unique interpolation

algorithm that works for all potential routes in the nonattainment area. However, the developed algorithm allows any route within the nonattainment area. The user puts in the coordinates of the route. The algorithm automatically applies the above procedure using the existing WRF-CMAQ data of episode 1 and determines an optimized interpolation equation set. This means for a grid-cell for which the interpolation is to be made, the coefficients a_j and b change depend on the sniffer route. This approach provides high flexibility for future mobile measurements. It also can be transferred to other cities than Fairbanks (see Appendix C for a demonstration) and applied there to interpolate concentrations from mobile measurements if WRF-CMAQ data for construction of the interpolation equations are available.

In this study, we used the simulated $PM_{2.5}$-concentrations of episode 1 to develop the interpolation algorithm. We used the simulated $PM_{2.5}$-concentration of episode 2 to evaluate the accuracy of the obtained interpolation algorithm.

As wind patterns affect the spatial distribution of $PM_{2.5}$ over the nonattainment area [*Tran and Mölders*, 2011], it was proposed to include wind direction in the interpolation algorithm. We developed an interpolation equation like Eq. (1) for each of the 8 wind direction sectors of 45°. Since the objective of the interpolation is to provide public air quality advice, it must be performed as soon as possible after a sniffer drive is completed. Therefore, the wind field observed at the meteorological (MET) tower that is located in downtown Fairbanks was selected as the point from where to take the wind direction information. The FNSB namely has immediate access to these measurements. Other sites with wind direction in Fairbanks do not provide wind direction data instantly; therefore data from these sites is not useful for the intended task.

Again, we used WRF-CMAQ simulated data of episode 1 to develop the interpolation algorithms, but this time with consideration of the wind direction. We evaluate the performance of the wind direction sensitive algorithm with the WRF-CMAQ simulated data obtained from episode 2. We compared the interpolated concentration distributions obtained with (WWD) and without (NWD) wind direction-classification and investigated their accuracy. The results showed that the algorithm without consideration of wind direction provided better results than those with consideration of wind direction.

Investigation showed that the MET tower wind direction data are not representative for the nonattainment area. On many days, winds come from other directions at the airport, Eielson and Fort Wainwright site than observed at the MET tower. Examination of six months of WRF/Chem data showed that especially on days with relatively low wind speeds (<1m/s) wind comes from various directions in the nonattainment area. Thus, we rejected the inclusion of wind direction data into the algorithm. In the following, always the algorithm without consideration of wind direction will be used and results from this algorithm are discussed if not mentioned explicitly otherwise.

CHAPTER 2 - FINDINGS

2.1 WRF-CMAQ Performance Evaluations

WRF-CMAQ's performance in predicting the meteorological quantities was slightly better for episode 2 than episode 1 (Table 2). Throughout both episodes, WRF-CMAQ consistently predicted warmer and drier near-surface conditions, higher 10m wind-speeds and lower daily accumulated downward shortwave radiation than observed (Fig. 6, 7). Note that WRF is known to overestimate wind speed under stagnant weak wind (<1.5m/s) weather conditions [*Zhao et al.*, 2011; *Mölders et al.*, 2012].

The temporal evolutions of 2m-temperature, 2m-dew-point temperature, wind-speed and sea-level pressure were well captured (Fig. 6). WRF-CMAQ also well captured the spatial variations of these quantities. Note that in both episodes there were only two sites having observed pressure data. WRF predicted wind direction with a mean bias <30°. This falls within the range of other WRF and model studies for this region [*Mölders*, 2008, 2010, *Yarker et al.*, 2010; *Mölders et al.*, 2011a, 2012].

Table 2. Performance skill-scores of WRF-CMAQ in predicting 2m-temperature (T), relative humidity at 2m (RH), 10m wind speed (v), accumulated downward shortwave radiation (SW), sea-level pressure (SLP), and 2m-dewpoint temperature (T_d) in episode 1 (normal print) and episode 2 (*italic*). Here STDEV is the standard deviation.

| Quantity	Bias	RMSE	SDE	R	Mean simulated	Mean observed	STDEV simulated	STDEV observations
T (^{o}C)	4.69	7.39	5.71	0.766	-17.48	-22.16	8.2	8.46
	1.68	*5.11*	*4.82*	*0.891*	*-16.92*	*-18.6*	*9.01*	*10.6*
RH (%)	-17	24	16	0.267	56	73	15	12
	-15	*23*	*17*	*0.290*	*57*	*73*	*16*	*14*
v (m/s)	1.43	2.09	1.52	0.667	2.47	1.04	2.03	1.5
	1.47	*2.13*	*1.54*	*0.568*	*2.58*	*1.11*	*1.84*	*1.33*
SW (Wm^2)	-33	242	240	-0.248	78	111	48	224
	~0	*265*	*265*	*-0.167*	*140*	*140*	*86*	*237*
SLP (hPa)	-2.18	3.64	2.88	0.845	1017.14	1019	4.58	5.42
	-1.03	*3.32*	*3.15*	*0.988*	*1018.97*	*1020*	*18.89*	*19.67*
T_d (^{o}C)	-0.1	8.9	8.9	0.651	-24.6	-24.6	9.3	11.4
	-1.9	*5.4*	*5.1*	*0.890*	*-23.7*	*-21.8*	*10.6*	*11.0*
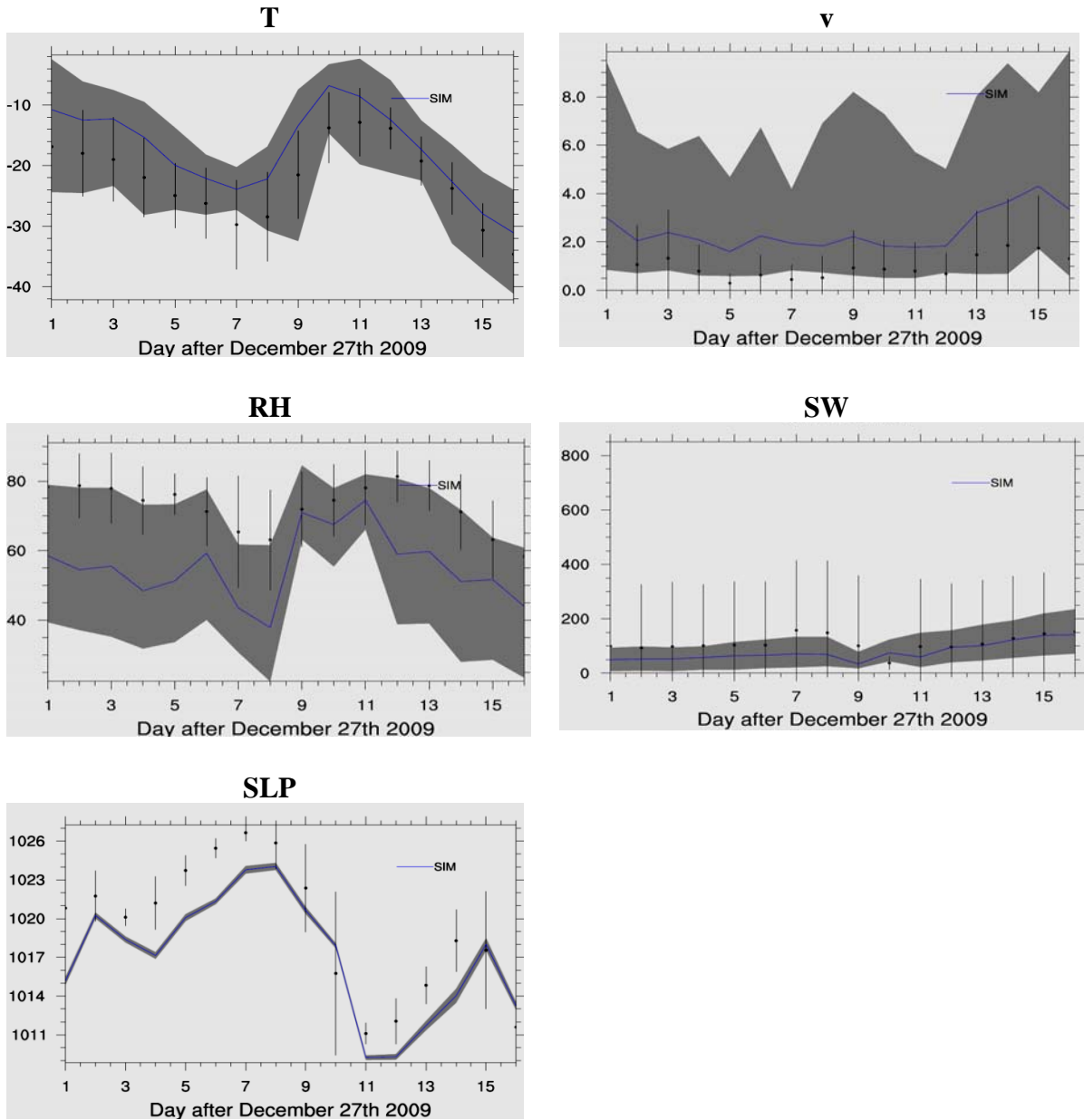
Fig. 6. Temporal evolution of daily averaged air-temperatures T (^{o}C), wind-speed v (m/s), relative humidity RH (%), daily accumulated downward shortwave radiation SW (W/m^2), and sea-level pressure SLP (hPa) averaged over the 14 observational sites for which data was available in episode 1. Solid blue line and closed circles indicate simulated and observed quantities; grey-shading and vertical bars indicate the variance of the simulated and observed quantities, respectively
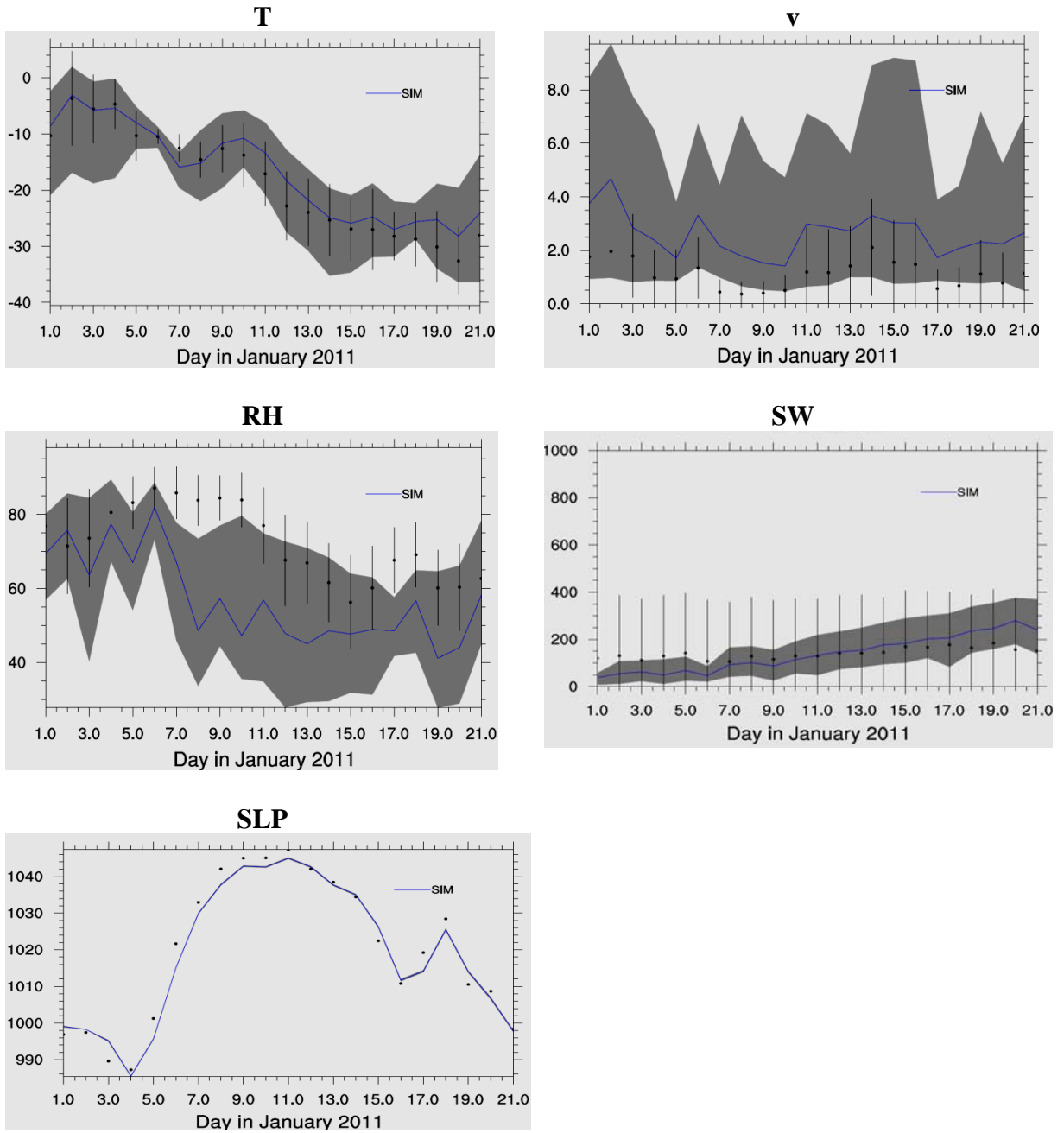
Fig. 7. Like Fig. 6, but for all 18 observational sites for which data was available during episode 2.

For both episodes, WRF-CMAQ simulated the $PM_{2.5}$-concentrations at the State Office Building site better than at other sites. The R, mean bias and RMSE of the 24h-average $PM_{2.5}$-concentrations obtained at the SB site are 0.481 (0.707), -2.8 (7.3)$\mu g/m^3$, 12.1 (12.2)$\mu g/m^3$ in episode 1 (2).

For each episode, we examined the time needed for spin-up of the chemical fields. For episode 1 (2) the spin-up time was 3 (5) days. The results from these spin-up days were discarded from the analysis.

For episode 1, WRF-CMAQ captured all but two observed exceedances at the SB site (Fig. 8). From December 27 to 31, 2009, the temporal evolution of hourly $PM_{2.5}$-concentrations was acceptably captured. The peak of predicted $PM_{2.5}$-concentration was predicted about 5 hours ahead of the observed time. On the remaining days, the temporal evolution was well captured.
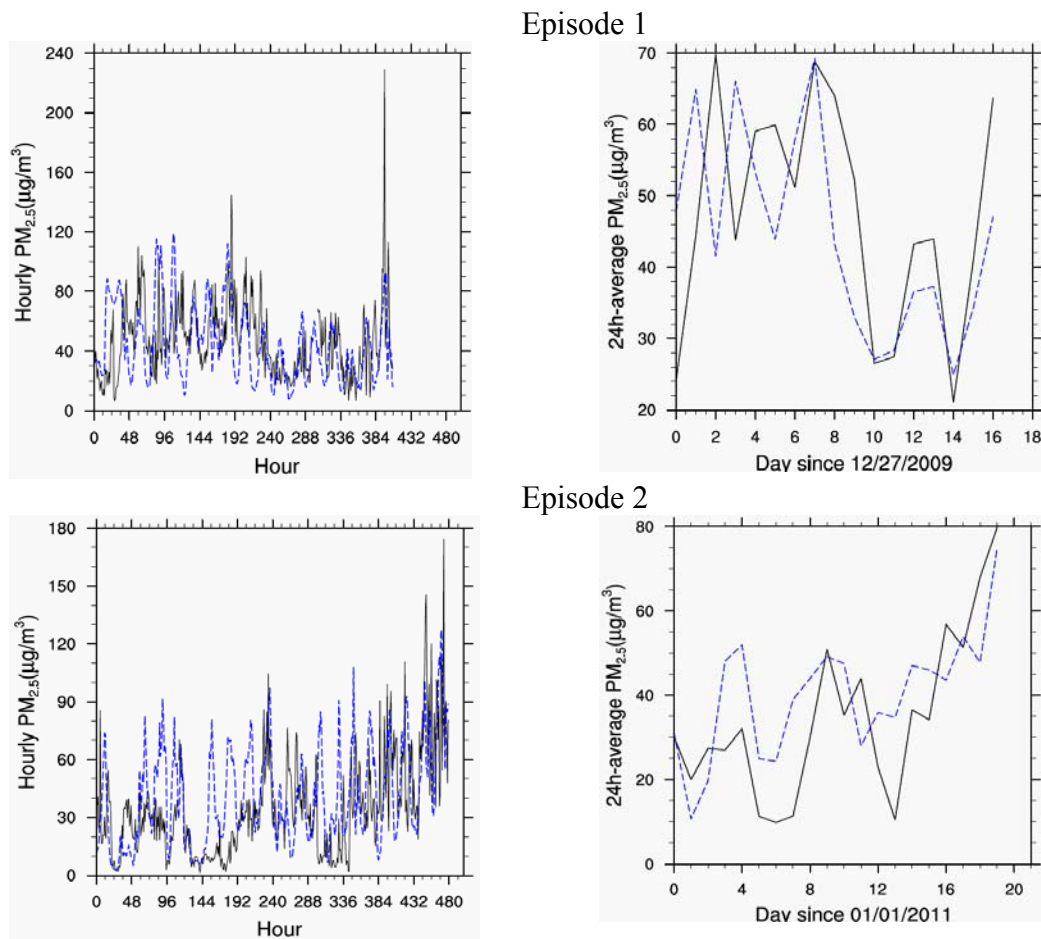
Episode 1

Episode 2

Fig 8. Temporal evolution of simulated and observed (left) hourly and (right) 24h-average $PM_{2.5}$-concentrations as obtained at the SB site for episode 1 (upper part) and 2 (lower part). Dashed blue and solid black lines indicate simulated and observed quantities, respectively.

To examine whether errors in the emissions were the cause we performed a simulation for the first 5 days with modified emissions by shifting the temporal allocation functions to 5 hours later in accordance to the above finding. However, the performance of this sensitivity simulation was not better than for the reference simulation. Therefore, we concluded that this

17

offset was caused by the simulated meteorology and effects of initial conditions rather than by the emissions. Note that such mistiming frequently occurs with WRF [*Mölders*, 2008; *Mölders et al.,* 2010; 2011a, 2012] and other mesoscale models.

The results obtained for episode 2 showed a better performance of WRF-CMAQ with respect to predicting PM$_{2.5}$-concentration at the SB site than in episode 1 (Fig. 8). WRF-CMAQ captured all except one exceedance at the SB site. However, WRF-CMAQ predicted 5 exceedances that were not observed. The relatively strong overestimation of PM$_{2.5}$ that occurred between January 7 and 9, 2011 may be due to the fact that WRF-CMAQ simulated much drier conditions than observed (Figs. 7, 8).
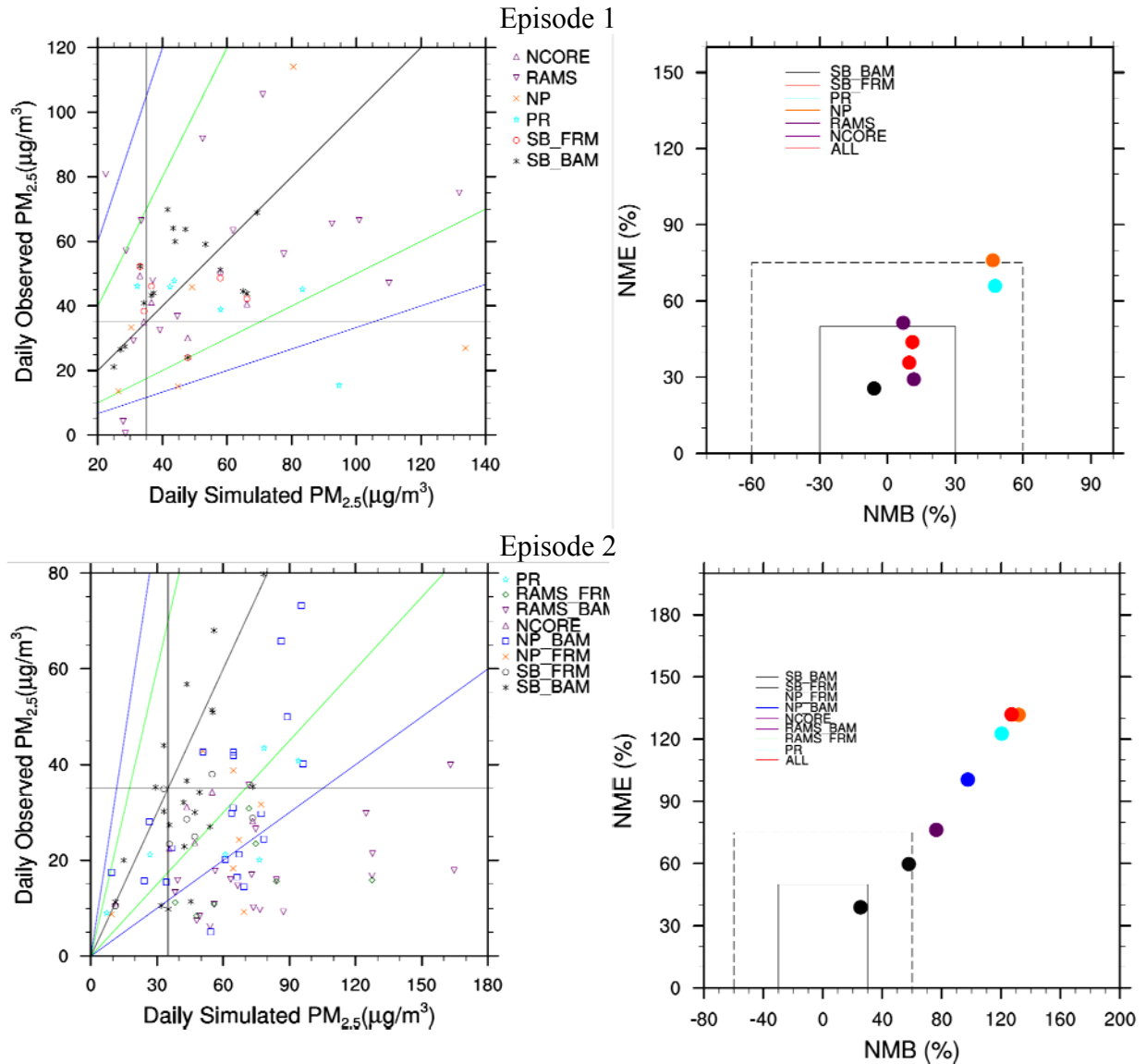
Episode 1

Episode 2

Fig 9: Scatter (left) and soccer (right) plots of simulated and observed 24h-average PM$_{2.5}$–concentrations at the monitoring sites for which data was available during episode 2. The black, green and blue lines in the scatter plots indicate the 1:1-line and a factor of two and three agreement between pairs of simulated and observed values, respectively.

Overall, WRF-CMAQ performed better in predicting the PM$_{2.5}$-concentrations for episode 1 than episode 2. Overall sites and days, the mean bias, RMSE, R and FAC2 of 24h-average PM$_{2.5}$-concentrations in episode 1 are 3.8μg/m^3, 28.9μg/m^3, 0.219 and 91%, respectively. In episode 2, the corresponding values are 32.8μg/m^3, 34.3μg/m^3, 0.204 and 44%, respectively. For episode 1, 66% and 100% of the pairs of simulated and observed PM$_{2.5}$-concentrations from all stationary sites fell within the EPA recommended goals and criteria of performance. In episode 2, only the pairs of simulated and observed PM$_{2.5}$-concentrations at the SB site fell within the goal of performance, and 37% of the pairs were within the performance criteria. Note that the performance goals denote to performance that is the best a state-of-the-art model can reach and the performance criteria indicates the performance a model should have to be accepted for regulatory applications [*Boylan and Russell*, 2006].

In episode 2, WRF-CMAQ overestimated the 24h-average PM$_{2.5}$-concentrations at NP and the RAMS sites by two orders of magnitude. Uncertainty in the observed data and spatial allocation of emissions, as well as errors in the meteorological predictions are the causes. *Mölders et al.* [2012] assessed that up to 24% of the normalized mean error can be explained by measurement errors at the extremely low temperatures as they occur in Fairbanks. On average over episode 1 and all sites, the 24h-average PM$_{2.5}$-concentrations have a fractional bias and error, and a normalized mean bias and error of 13%, 42%, 11% and 44%, respectively. On average over episode 2 and all sites, the 24h-average PM$_{2.5}$-concentrations have a fractional bias and error, and a normalized mean bias and error of 72%, 77%, 128% and 134%, respectively.

The scores for episode 1 are slightly better than the scores found by *Mölders et al.* [2012] on average over half-a-year and all sites. They obtained a fractional bias and error, and a normalized mean bias and error of 22%, 67%, 13% and 71%, respectively, for the 24h-average PM$_{2.5}$-concentrations. The scores for episode 2 are worse than the scores found by *Mölders et al.* [2012] on average over half-a-year and all sites. Investigation showed that the weaker performance in episode 2 than 1 is mainly related to the RAMS observations. There had been repeatedly problems with the RAMS in the past [*Conner* 2009; pers. comm.]. Thus, the actual WRF-CMAQ performance in predicting PM$_{2.5}$-concentrations in episode 2 may be better than it seems from the skill scores.

Table 3. Skill-scores of WRF-CMAQ evaluated with sniffer data in episode 1 (normal) and episode 2 (italic).

Quantities	Bias	RMSE	R	Mean WRF-CMAQ	Mean observations	STDEV WRF-CMAQ	STDEV observations
T	9.1 *4.5*	9.9 *6.1*	0.851 *0.909*	-17.6 *-21.5*	-26.7 *-25.9*	7.6 *7.3*	6.5 *9.3*
PM$_{2.5}$	3.1 *11.3*	53.5 *41.3*	0.097[*] *0.156[*]*	41.3 *40.2*	38.2 *28.9*	43.9 *33.9*	35.0 *26.7*

[*]Correlation is not statistical significant at the 95% level of confidence.

Skill-scores of simulated $PM_{2.5}$-concentrations and temperatures along the sniffer routes in comparison with the $PM_{2.5}$-concentrations and temperatures measured by the sniffer are presented in Table 3. In general, WRF-CMAQ consistently overpredicted temperatures (Figs. 10, 11). The WRF-CMAQ warm bias was stronger in episode 1 than in episode 2. WRF-CMAQ failed to capture the extreme low temperatures ($<-35^{o}C$) measured at some locations by the sniffer. This behavior is due to the fact that the sniffer can capture large temperature gradients between the valley and the hills whereas in the model, the simulated temperature represents the volume-average temperature for an entire grid-cell of $1.3\times1.3km\times8m$. Similar was found by *Mölders et al.* [2012] in the six month WRF/Chem evaluation by means of mobile temperature measurements. In both episodes, WRF-CMAQ overestimated the $PM_{2.5}$-concentrations.

Table 4. Skill scores as obtained at various sites.

| Site	FB (%)	FE (%)	NMB (%)	NME (%)	FAC2 (%)	# of observations
Episode 1						
All sites	13	42	11	44	91	58
SB_BAM	-5	26	-6	26	100	17
SB_FRM	8	35	10	36	100	6
NP	43	58	47	76	67	6
NCORE	9	27	12	29	100	6
PR	31	42	47	66	83	6
RAMS_BAM	15	58	7	51	77	17
Episode 2						
All sites	72	77	128	134	44	96
SB_BAM	28	40	25	39	81	21
SB_FRM	38	40	58	60	86	7
NP_FRM	74	74	132	132	43	7
NP_BAM	64	71	98	101	48	21
PR	58	66	120	123	50	6
NCORE	47	47	76	77	83	6
RAMS_BAM	129	129	377	377	0	21
RAMS_FRM	123	123	330	330	0	7
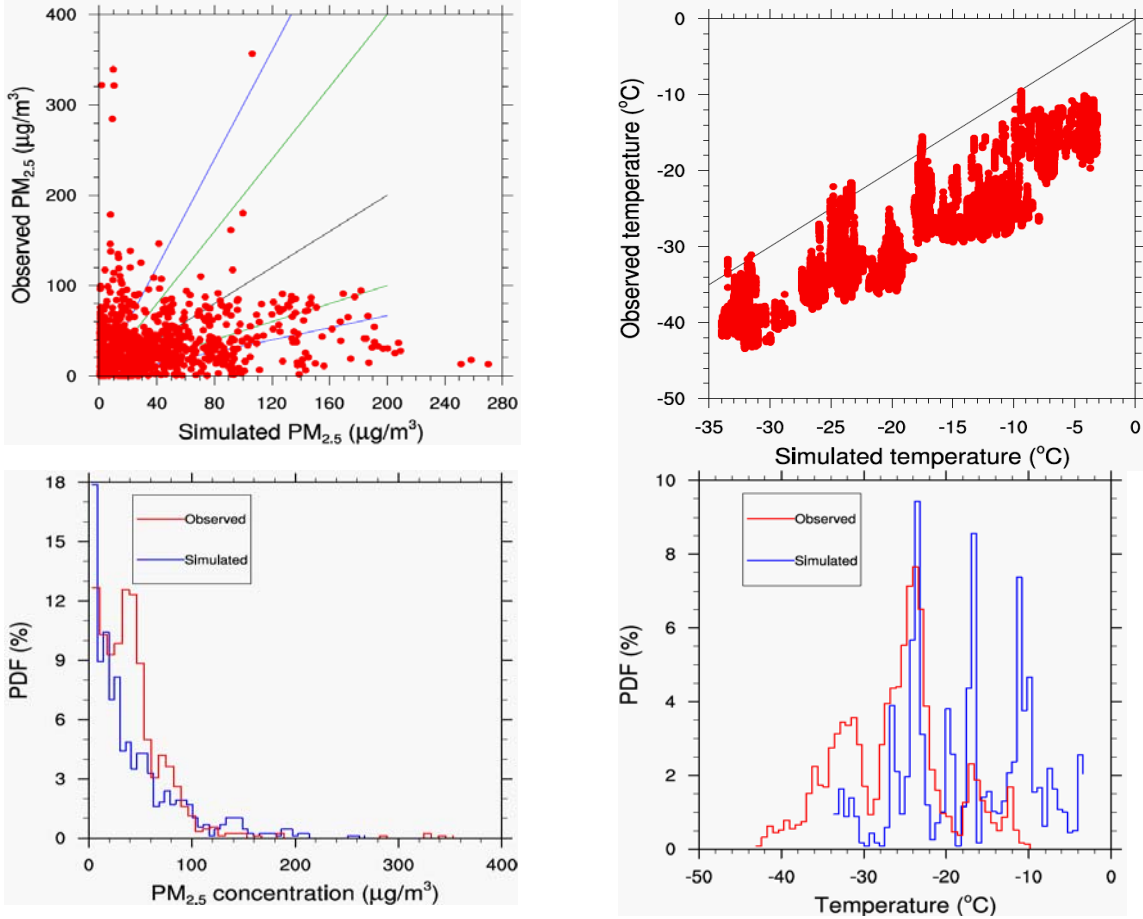
Fig. 10. Scatter plots (upper part) and population distribution plots (lower part) of simulated temperatures and PM$_{2.5}$-concentrations vs. temperatures and PM$_{2.5}$-concentrations measured by the sniffer for all sniffer drives during episode 1.
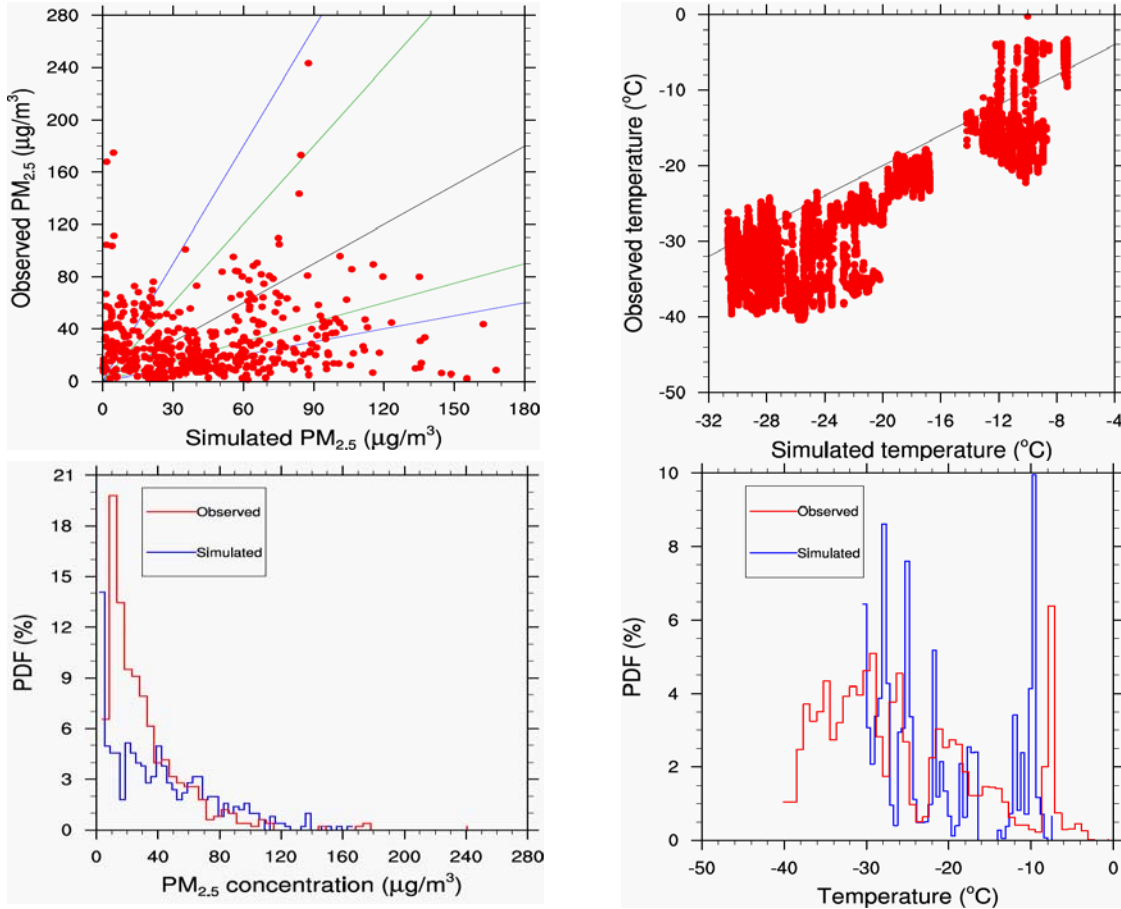
Fig. 11. Like Fig. 10, but for all sniffer drives during episode 2.

2.2 Traffic Emissions

Over all two episodes, the traffic emissions contribute 7% and 2% to the total $PM_{2.5}$-emissions on average over the domain and over the nonattainment area, respectively. Outside the nonattainment area, traffic is the largest contributor to $PM_{2.5}$-emissions. In the nonattainment area, the contribution of traffic to the total $PM_{2.5}$-emissions varied with source activities. Traffic emissions contributed about 2, 2, 3, and <1% of the total $PM_{2.5}$-emissions on average over the City of Fairbanks (FC), Fort Wainwright (FW), North Pole (NP) and the hills (HL) (see Fig. 13 for locations). In downtown Fairbanks (DT), traffic emissions made up about 3% of the total $PM_{2.5}$-emissions. In the nonattainment area, traffic emissions made up about 50%, <1%, 22%, 17% to the total emissions of CO, SO_x, NO_x, and volatile organic compounds (VOC), respectively.
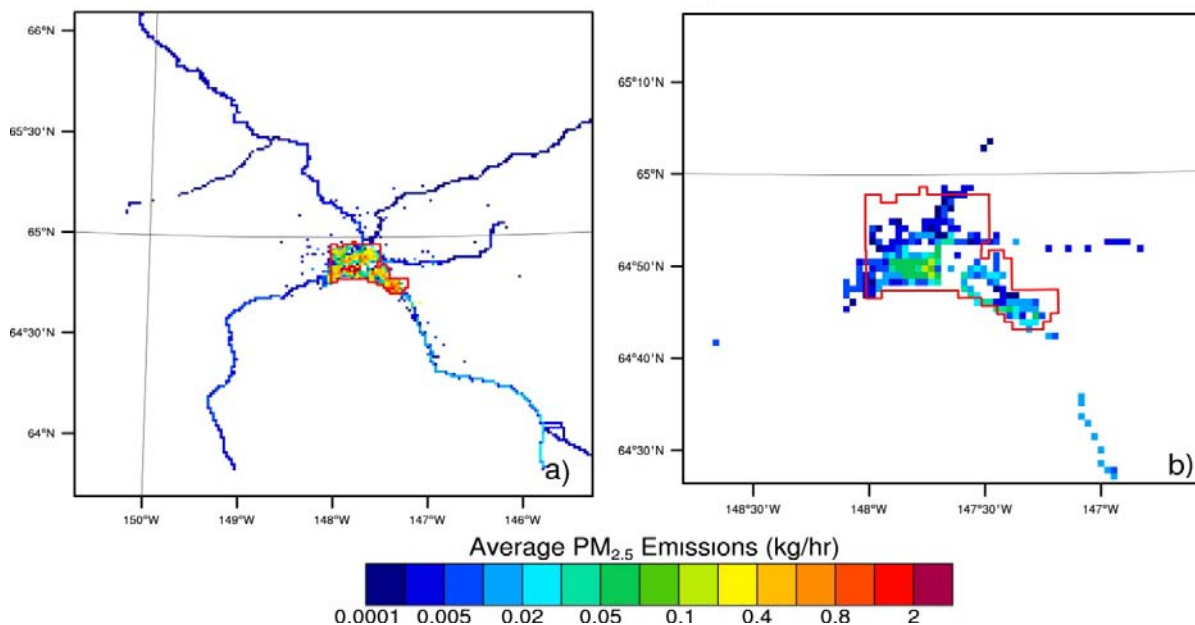
Fig. 12. Average PM$_{2.5}$-emissions in REF (left) and zoom-in on the PM$_{2.5}$-emissions differences (REF-NTE) for episode 1. The red polygon indicates the Fairbanks PM$_{2.5}$-nonattainment area. Similar emission patterns were found for episode 2 (not shown).

2.3 Impact of Traffic Emissions

The impacts of traffic emissions on the PM$_{2.5}$-concentrations marginally differ between episode 1 and 2. The distribution of the 24h-average PM$_{2.5}$-concentrations varied strongly among regions (Figs. 13, 14). The 24h-average PM$_{2.5}$-concentrations were 36.3 (34.9), 25.8 (27.3), 26.3 (25.9), and 5.6 (8.34) µg/m^3 on average over FC, NP, FW and in the HL, respectively in episode 1 (2). In DT, the 24h-average PM$_{2.5}$-concentration was 84 (76.4) µg/m^3 on average in episode 1 (2). Most of grid-cells that frequently experienced high 24h-average PM$_{2.5}$-concentrations (>100µg/m^3) are located in FC. These findings imply that the spatial distribution of PM$_{2.5}$-concentrations was relatively consistent in the two episodes.

On average over the nonattainment area and episode 1, the 24h-average PM$_{2.5}$-concentrations were 24.0 and 21.5µg/m^3 in REF and NTE, respectively. These spatio-temporal averages would equal to about 10% reduction ((REF-NTE)/REF) of the 24h-average PM$_{2.5}$-concentrations, on average, if no traffic emissions had occurred. This means traffic contributed about 10% to the 24h-average PM$_{2.5}$-concentrations on average over the nonattainment area and time in the episode 1. The corresponding values for episode 2 are 24.4 and 22.3µg/m^3, and about 9% reduction, respectively. Highest 24h-average PM$_{2.5}$-differences (REF-NTE) obtained on any day in episode 1 and 2 were 24.0 and 20.0µg/m^3, respectively.

In episode 2, the amount of PM$_{2.5}$-reduction is about the same as in episode 1 in FC, FW, NP and DT, i.e. 10-12% on average. In the HL, the PM$_{2.5}$-reduction was 4.5% and 1% in episode 1 and 2, respectively. Given that traffic emissions only contributed less than 1% to the total PM$_{2.5}$-emissions in this area, the PM$_{2.5}$-reduction in this area seems to be heavily governed by the reduction in other areas of the nonattainment area.

23

In the nonattainment area during episode 1 (2), the highest 24h-average $PM_{2.5}$-concentration on any day was 274.4 (213.5) $\mu g/m^3$ and 257.1 (193.5) $\mu g/m^3$ in REF and NTE, respectively.

The average relative response factor to "no traffic" obtained at the State Office Building site is 0.87 (0.88) in episode 1 (2). The highest RRF obtained at any time at this site is 0.82. The highest RRF for polluted grid-cells (24h-averaged $PM_{2.5}$-concentration >35$\mu g/m^3$ on average) in the nonattainment area was 0.68 (0.75) in episode 1 (2). At these grid-cells, an RRF of ~1 also occurred on several days.
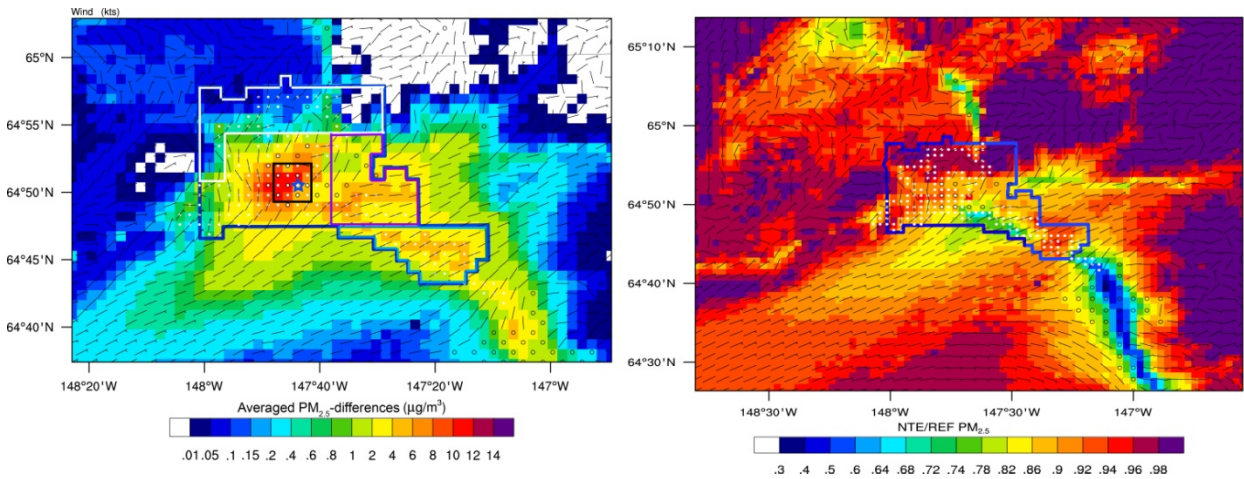

Fig. 13. Zoom-in on the average $PM_{2.5}$-differences REF-NTE (left) and the average RRF (NTE/REF) for episode 1 with wind barbs superimposed. The nonattainment area, grid-cell holding the official monitoring site at the State Office Building and grid-cells traveled by instrument vehicle are represented by the blue polygon, blue star and white dots, respectively. North Pole (NP), Fort Wainwright (FT) and hills (HL) regions are represented by cyan, purple and white polygons, respectively, and the remaining region is Fairbanks City (FC). Downtown area (DT) is indicated by the black square. Note that these lines are not the administrative boundaries.
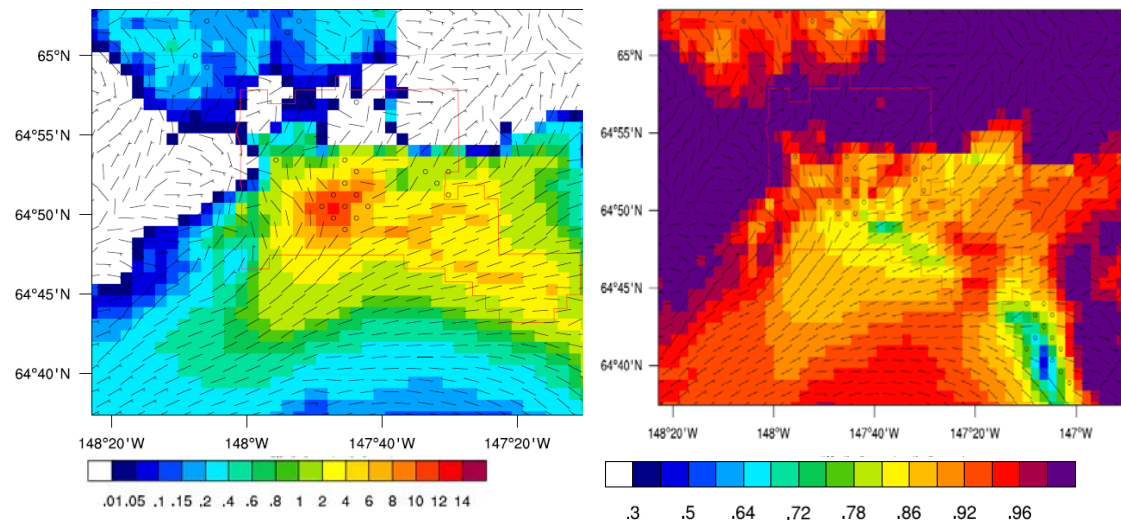

Fig. 14. Like Fig. 13, but for episode 2.

Exceedances occurred on all days in both episodes and no exceedance-day was avoided in NTE as the 24h-average PM$_{2.5}$-concentrations were high throughout all days of the episodes. There were 1450 (1930) exceedances that occurred at any grid-cell in the nonattainment area at any day in REF and 229 (237) of them were avoided in NTE in episode 1 (2). At the SB site, 3 (3) exceedances were avoided in NTE in episode 1 (2).
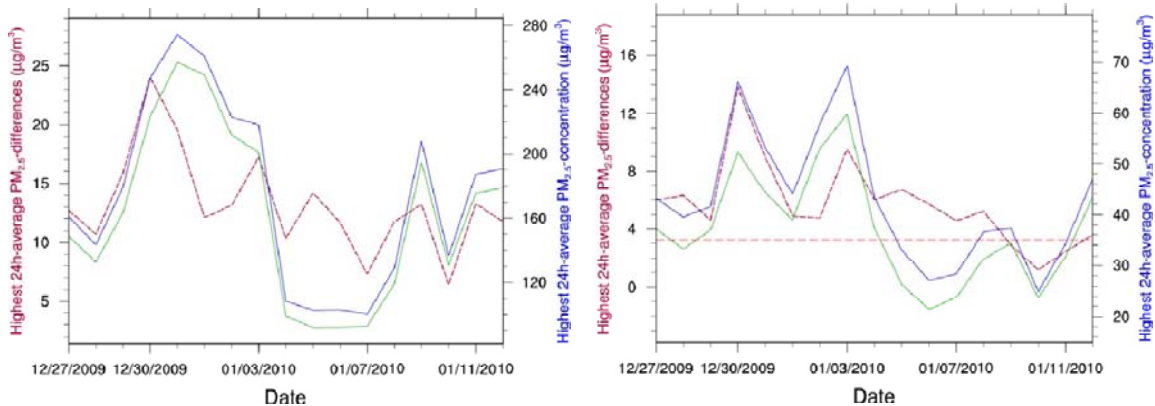

Fig 15: Highest 24h-average PM$_{2.5}$-concentrations in REF (blue line) and in NTE (green line), and highest 24h-average PM$_{2.5}$-difference (dash red line) as obtained (left) on average over the nonattainment area and (right) at the SB site in episode 1.
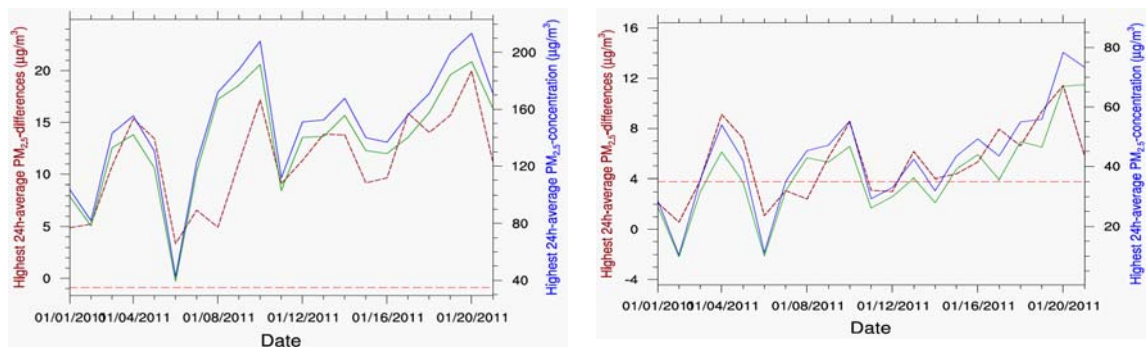

Fig 16: Like Fig. 15, but for episode 2.

3.4 PM$_{2.5}$ Interpolation

We used the results of the simulation with consideration of traffic emissions for episode 2 to assess the general applicability of the interpolation algorithm. Recall that the algorithm was developed based on the simulation results of episode 1. Again we used the WRF-CMAQ data as the "grand truth", i.e. as proxy for an actual situation. We determined the 24h-average PM$_{2.5}$-concentrations from the simulation results of episode 2 along an arbitrarily chosen sniffer route. These concentrations were plugged into the interpolation algorithm that

determined the linear regression equations (Eq. (1)) based on the route data and calculated the interpolated concentrations based on the concentration along the route.

The comparison of interpolated and simulated PM$_{2.5}$-concentration of episode 2 revealed that the performance of the interpolation algorithm depends on the sniffer route. The performance is worst when the "assumed" sniffer only covered a few grid-cells, or when the assumed route was heavily oriented to one side of the nonattainment area, for instance, just in North Pole or in the hills (cf. Figs. 17, 18).
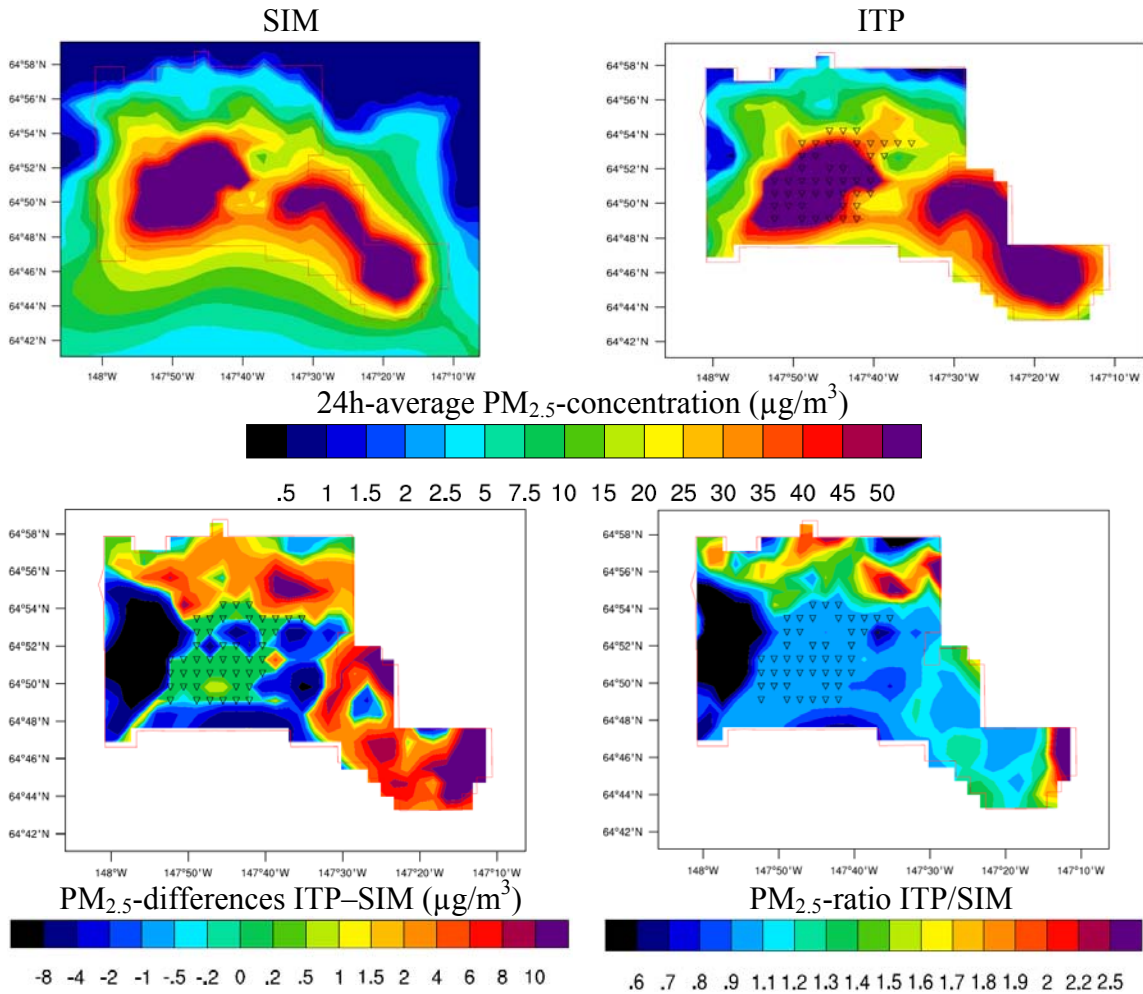

Fig. 17. Interpolated (ITP) vs. simulated, i.e. "grand truth" (SIM) PM$_{2.5}$-concentrations as obtained with the developed interpolation algorithm using the WRF-CMAQ data for 01/11/2011 as "proxy" for observation in the nonattainment area. The black triangle indicates the grid-cells of the assumed sniffer route on this day.
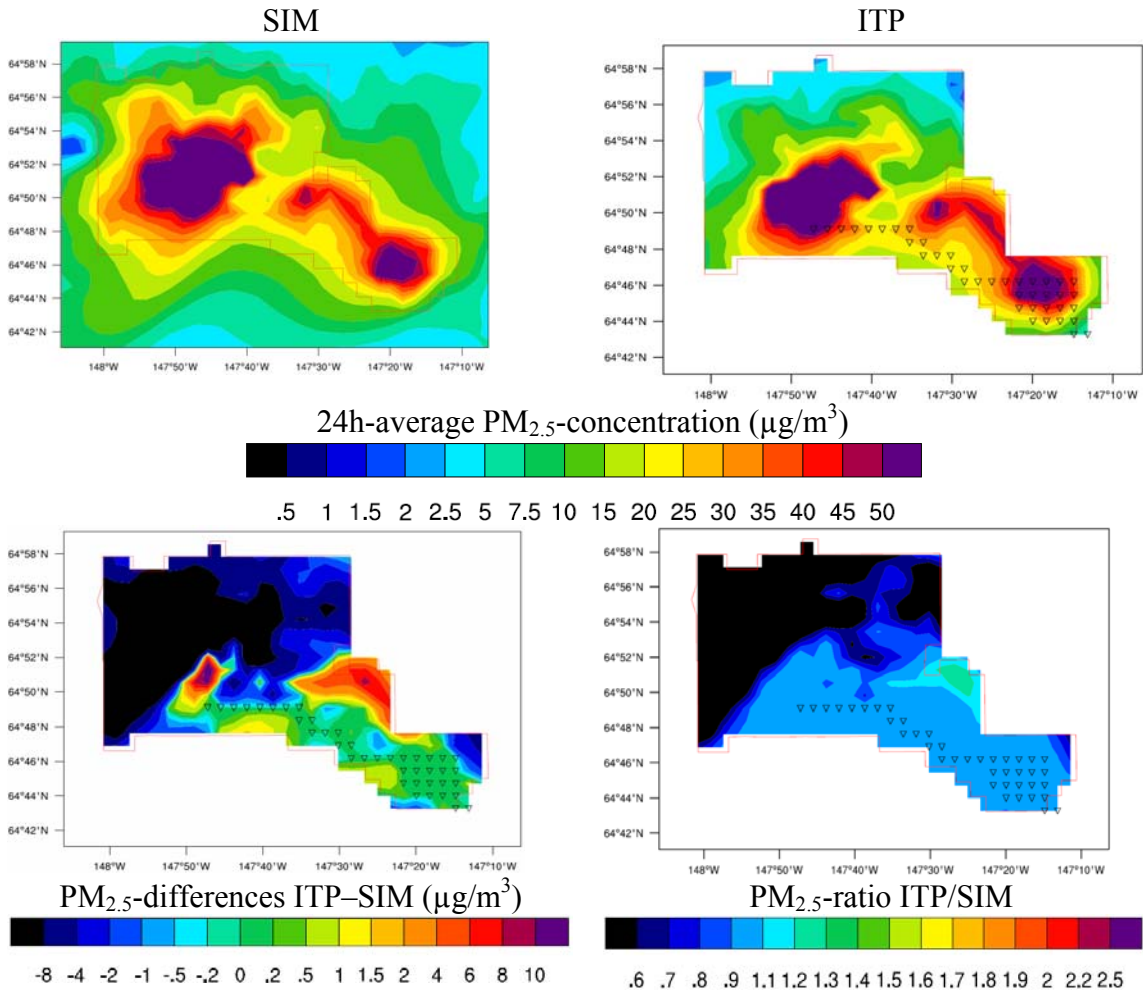
Fig. 18. Like Fig. 15, but for 01/18/2011.

For episode 2 the assessment of the overall performance of the interpolation algorithm leads to the following skill scores for grid-cells adjacent to grid-cells covered by the sniffer route: R>0.8, NMB<20% and NME<20% (Fig. 19). The performance is lower in the hills than else where in the nonattainment area. However, since PM$_{2.5}$-concentrations are usually below the NAAQS in the hills, this lower performance does not lead to false alarms, i.e. a notification that the air would be unhealthy.

To demonstrate that inclusion of wind direction is disadvantageous we also assessed the interpolation algorithm that considered wind direction (WWD). The lower performance of WWD than the recommended interpolation algorithm without wind direction consideration (NWD) (cf. Figs. 19, 20) is due to the fact that the wind direction measured at the MET tower does not represent the wind pattern over the nonattainment area well. Therefore, we rejected the inclusion of wind direction.
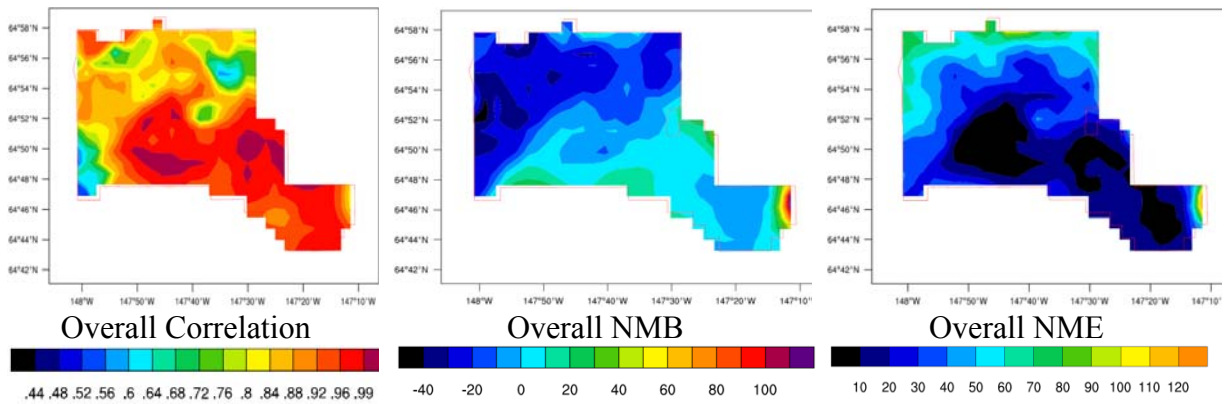
Fig. 19. Overall performance of the recommended interpolation algorithm (without consideration of wind direction) as obtained for episode 2.
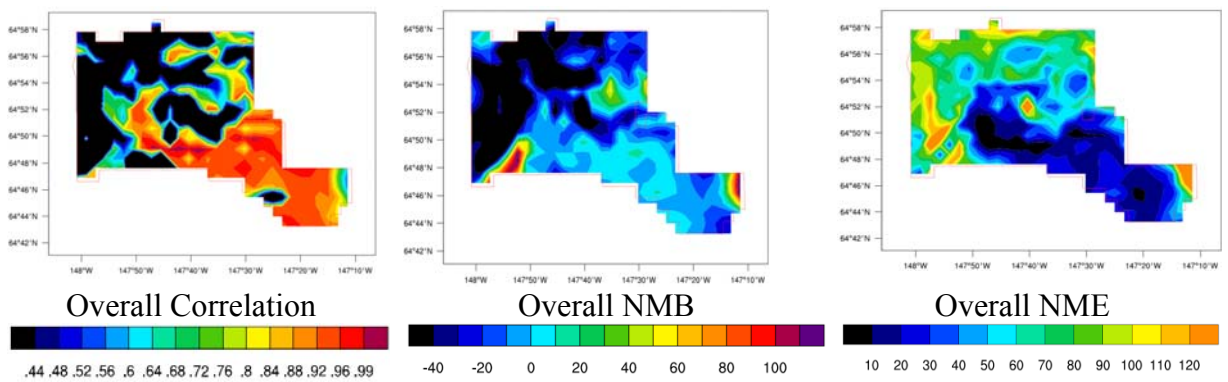
Fig. 20. Like Fig. 19, but for the interpolation algorithm with consideration of wind direction.
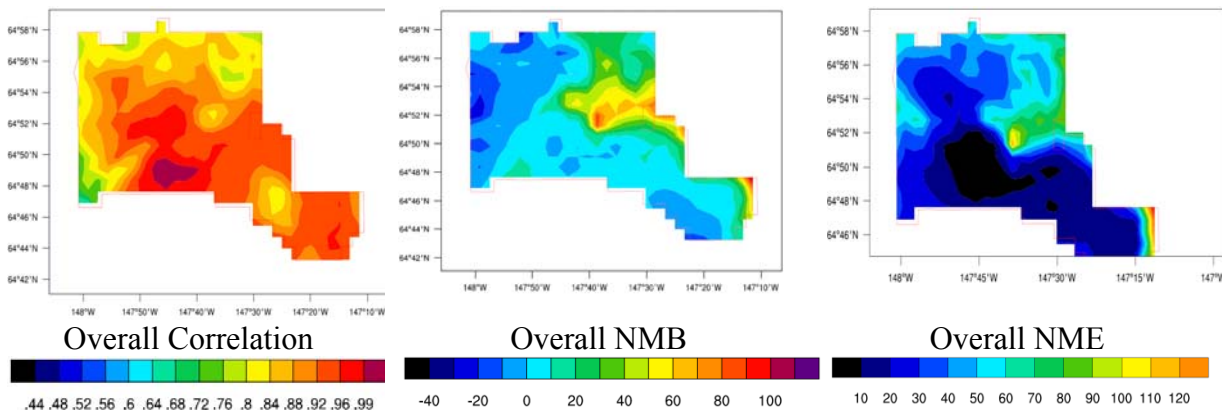
Fig. 21. Like Fig. 19, but for the 100 random samples.

The above described assessment suggested that the accuracy of the interpolation algorithm is route dependent. Therefore, we examined the accuracy of the algorithm for various randomly chosen, but possible routes for the 21 days of episode 2. In doing so, we randomly picked one day of episode 2 and one possible route. By using the WRF-CMAQ provided PM$_{2.5}$-concentrations of that day and along the selected sniffer route, we constructed Eq. (1), and interpolated the concentrations into the areas outside the assumed route. We repeated this procedure 100 times. We then compared these 100 interpolated PM$_{2.5}$-concentration datasets with the corresponding WRF-CMAQ PM$_{2.5}$-concentrations that again were assumed as the

28

"grand truth". The comparison between the interpolated and simulated PM$_{2.5}$-concentrations led to R>0.720, -30%<NMB<60% and NME<100% for most locations in the nonattainment area on average overall 100 arbitrarily chosen samples (Fig. 21).

As stated before, the interpolation performance was found to heavily dependent on the sniffer route. Therefore, we investigated whether we can identify a recommended route that would provide best interpolation performance no matter what the conditions are, i.e. on any day. The ultimate goal was that the recommended route would archive highest R values and lowest absolute NMB and NME in comparison with all other routes. In addition, the route must fulfill the following criteria:

1. The route should be as short as possible.

2. The sniffer must travel through PM$_{2.5}$ "hot spot areas", i.e. areas that have high potential for woodstove burning activity since the FNSB is interested in using the sniffer data to assess the benefit of their woodstove changeout program [*Swengaard* 2011; pers. comm.].

3. The travel plan must be reasonable and possibly with a minimum of redundancy in locations traveled. This optimization serves to avoid contradiction in results related to temporal fluctuations and allows for large coverage in the same amount of time.

We investigate various routes and selected the route that best satisfied the above criteria (Fig. 22). The overall performance of interpolation with this proposed route is better than the performance for any of the routes used in the above described random analysis (cf. Figs. 21, 23).
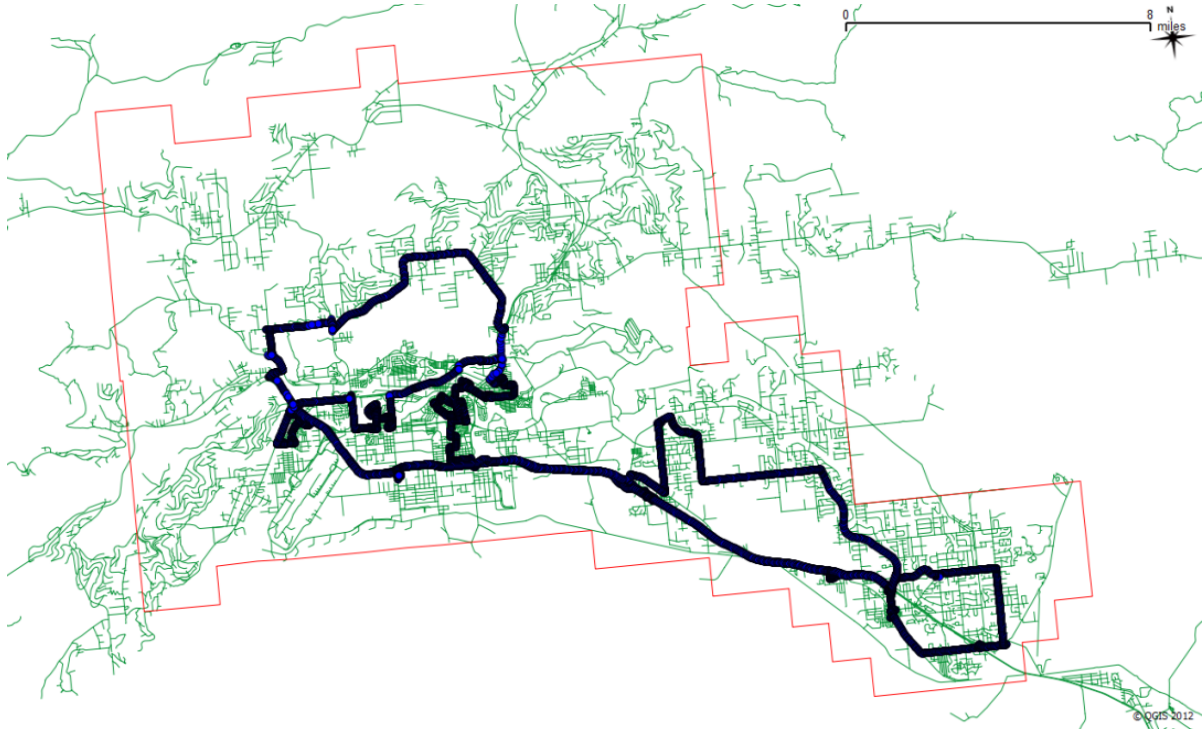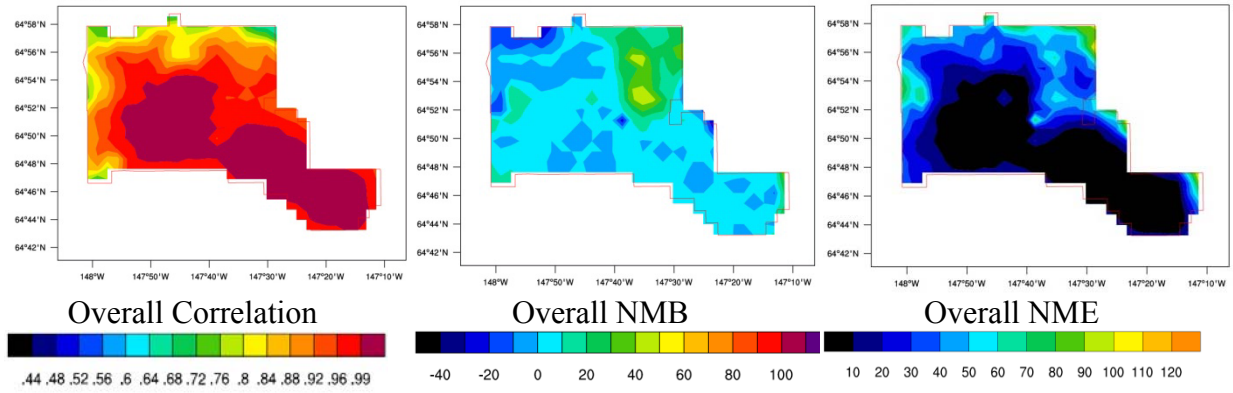

Fig. 22. Recommended sniffer route.

Fig. 23. Like Fig. 18, but for the recommended route.

CHAPTER 3 - INTERPRETATION, APPRAISAL, AND APPLICATIONS

3.1 General Recommendations

Our study was performed with the most current WRF-CMAQ version (4.7) available at the start of the project in its Alaska adapted form [*Mölders and Leelasakultum*, 2011]. This version is also used by Sierra Research for their simulations within the framework of the SIP. Our study showed that the modifications applied in the Alaska adapted WRF-CMAQ [*Mölders and Leelasakultum*, 2011] seem to be well suited for applications for the Fairbanks area for other episodes than tested by these authors. Meanwhile version 5.0 of CMAQ was released that allows for feedback between meteorological and chemical processes. This means changes in emissions may lead to changes in aerosol concentrations that lead to changes in radiation and cloud and precipitation formation processes. These changes in meteorological processes affect temperature, humidity and wind with consequences for scavenging, wet and dry deposition and photochemical reactions to just mention a few. Such features exist in the WRF/Chem [*Peckham et al.*, 2009]. WRF/Chem studies with these feedback processes showed that these aerosol-radiative feedback effects and the aerosol-cloud feedback effects may lead to notable differences in $PM_{2.5}$-concentrations even in Alaska [*Tran et al.*, 2011; *Leelasakultum et al.*, 2012]. Therefore, we recommend adapting the CMAQ version 5.0 for Alaska following *Mölders and Leelasakultum* [2011].

The performance evaluation showed that the Alaska adapted WRF-CMAQ [*Mölders and Leelasakultum*, 2011] performs well in simulating the $PM_{2.5}$-concentrations at the State Office Building site, but highly overestimates the $PM_{2.5}$-concentration at other stationary sites. On many days, simulated 24h-averaged $PM_{2.5}$-concentrations also suggested exceedances at the SB site that were lower in magnitude than in other areas. There were several days for which exceedances were simulated elsewhere in the nonattainment area, but not for the grid-cell holding the SB site. There are several reasons for this behavior:

1. Uncertainties in the annual emission of various emission sources.

2. Uncertainties in the spatial allocation functions of the emission inventory that led to too high allocation of emission in some areas, but to too low allocations in other areas.

3. Uncertainties in the observed $PM_{2.5}$-concentrations [cf. *Mölders et al.*, 2012]. Obviously, some difficulties exist with the devices at the extreme low Fairbanks temperatures [*Turner*, 2010; pers. comm.].

The $PM_{2.5}$-concentrations measured by the sniffer during the time of the two episodes showed some $PM_{2.5}$-concentration "hot spots" at the same or even higher order of magnitude than those observed at the same time at the SB site. One may conclude that the $PM_{2.5}$-concentrations measured at the SB site are not well representative for the overall exceedance conditions in the nonattainment area. These findings also agree with the results by *Mölders et al.* [2012] who analyzed all mobile measurements and fixed sites data made within November 2008 to March 2009. Reallocating the SB site and/or expanding the monitoring site network may be options to better capture those hot spots. Doing so may be helpful to better understand the situation in the nonattainment area.

This study showed that traffic emissions contributed about 10% to the $PM_{2.5}$-concentration in the Fairbanks nonattainment area. There were 3 exceedances that could have been avoided at the SB site in each episode if there had been no traffic emissions at all. We have to expect

that this number would be larger if the simulations would have been performed for an entire cold season (i.e. October to March).

Traffic is necessary and an automobile free nonattainment area cannot be enforced by law like it was on Sundays in Germany during the 1973 oil crisis. However, the fact that traffic emissions contribute about 10% on average to the $PM_{2.5}$-concentrations at the SB site suggests considering introducing gas as fuel for public transportation. In Europe in the 80s, this move led to many private car-owners having their vehicles refitted to run on natural car as there natural gas was cheaper than gasoline. Since the existing studies on the efficiency of emission-control measures indicate that a multi measure approach may be necessary to reach and retain compliance any additional reduction [*Mölders et al.*, 2011b] that can be easily made seems worth trying.

3.2 Application of the Interpolation Algorithms

The developed and assessed interpolation algorithm has been programmed as an NCAR Command Language (NCL) script. The WRF-CMAQ simulated data that serve as a database for the interpolation were created in netcdf format. How to apply the developed interpolation algorithm in the future is schematically shown in Figure 24. The NCL script and its associated WRF-CMAQ data can be easily transferred to another PC, Mac or other machine that operate under Unix. The only software packages that the potential user has to install are the NCL software and netcdf library. This software is freely available at http://www.ncl.ucar.edu/ and runs on all Unix systems. This means that potential users do not have to invest upfront in buying a software product.

The user also does not have to perform any WRF-CMAQ simulations. They use the data base that was created for the development of the algorithm. The input data are the mobile measurements. They have to be in the following format:

1. The text file contains data either in tab delimited or comma-separated format. The data must be organized into nine fields as follows:

Field 1: Date of measurements in YYYYDDD format where YYYY is the year and DDD is the Julian day

Field 2: Hour of measurements (0-23h format)

Field 3: Minute

Field 4: Second

Field 5: Latitudes of measurement points (in decimal)

Field 6: Longitudes of measurement points (in decimal)

Field 7: Elevations of measurement points (m)

Field 8: Measured temperature (^{o}C)

Field 9: Measured $PM_{2.5}$-concentration ($\mu g/m^3$)

2. Files may contain header lines and they must be preceded with the "#" sign

3. All missing values must be presented as -999 (blanks are not allowed). The NCL script only recognizes -999 as fill values for missing data.

4. A separate file is required for each sniffer drive

Example of a file that contains mobile measurement data is provided in Appendix B.

The output of the NCL program that is basically the interpolation algorithm procedure is a 2D-map of $PM_{2.5}$-concentrations in the nonattainment area. These concentrations are interpolated from the sniffer measurements. The user can chose whether they want the output as pdf or postcript format. This map can be used on the FNSB Air Quality Division's webpage for public air quality advisory purposes.
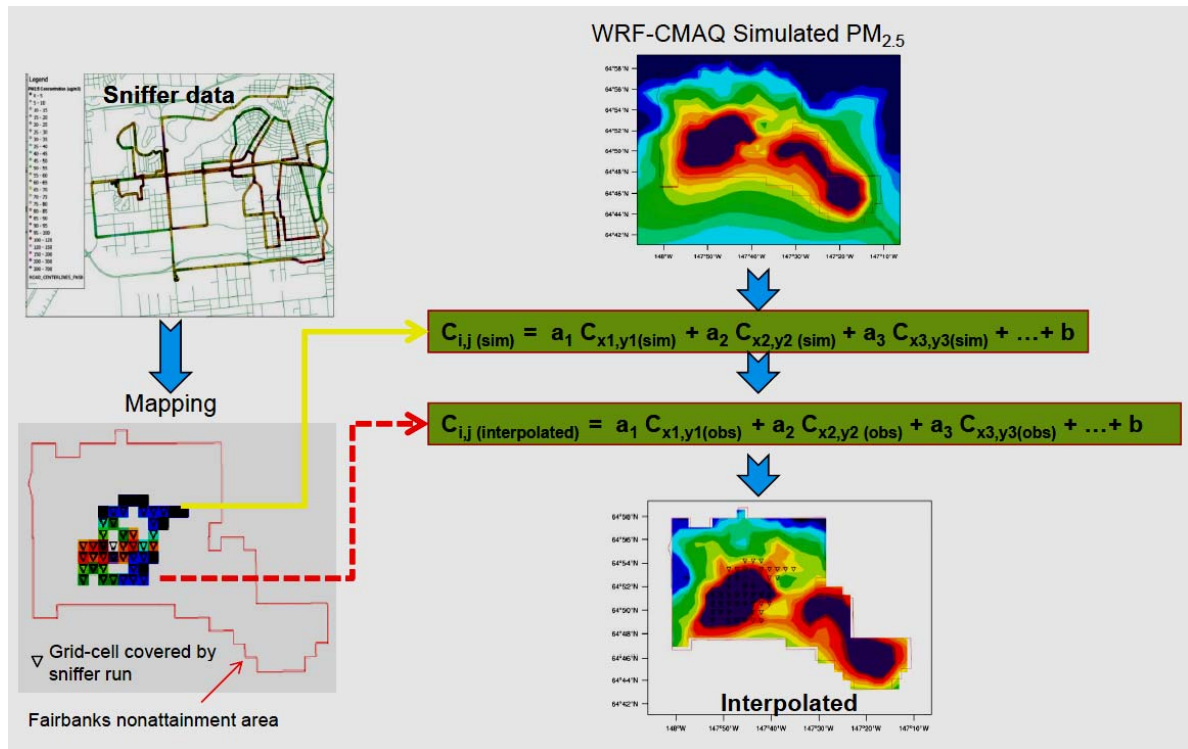

Fig. 24. Diagram of the data flow to obtain interpolated $PM_{2.5}$-concentration distributions from mobile measurements.

3.3 Broader Societal Impact

The public had frequently approached the FNSB that the Air Quality Division should provide a regionally differentiated air quality advisory. Our study developed a tool that permits to provide such service on days that matter.

The performance evaluations of episode 1 and 2 are an independent assessment of the Alaska adapted WRF-CMAQ model [*Mölders and Leelasakultum*, 2011] that is discussed to be considered for the SIP simulations. The evaluations made within the framework of our study enhance the trust into the Alaska adapted WRF-CMAQ and its results.

The study assessed the contribution of traffic emissions to the $PM_{2.5}$-concentrations at breathing level. The study provided improved knowledge on the impact of this important source. In Fairbanks, many people idle their cars. Thus, public information that traffic emissions contribute about 10% on average to the $PM_{2.5}$-concentrations at breathing level in the nonattainment area may change this behavior, and may help reduce traffic emissions and

improve air quality. Also the FNSB may consider opting for public advisory on highly polluted days to voluntarily not idle cars and voluntarily reduce driving to a minimum.

The WRF/Chem simulations for 2008 were evaluated by means of mobile $PM_{2.5}$-concentrations [*Mölders et al.*, 2012] within the framework of developing the QA/QC for this study. Note that these WRF/Chem simulations were the reference simulations made for the assessment of various emission-control measures tested by *Mölders et al.* [2011b].

CHAPTER 4 - CONCLUSIONS AND SUGGESTED RESEARCH

4.1 Conclusions

The Alaska adapted WRF-CMAQ [*Mölders and Leelasakultum*, 2011] has been successfully applied to simulate the meteorological conditions and $PM_{2.5}$-concentration for two episodes in winter 2009/10 and 2010/11. The evaluation of the performance of thesesimulations with observed meteorological data from 14 and 18 sites and $PM_{2.5}$-observations from 6 and 8 sites during episode 1 and 2, respectively, showed that this model setup provides acceptable results in simulating $PM_{2.5}$-concentration in the Fairbanks nonattainment area during these episodes.

Analyses of the results from simulations performed with and without consideration of traffic emissions showed that traffic emissions contribute about 10% on average to the $PM_{2.5}$-concentrations in the nonattainment area. However, the contributions differ in space and time. The average relative response factor obtained for the nonattainment area and the two episodes is 0.91. At the official monitoring site, the RRF is 0.87.

The accuracy of the interpolation algorithm developed within the framework of our study highly depends on the model performance and the sniffer route. The recommended route provides better interpolation results than all other routes tested. The developed interpolation algorithm is able to interpolate $PM_{2.5}$-concentrations measured by a sniffer into neighborhoods where no measurements were made. The results also showed that accounting for wind direction in the interpolation process is not beneficial in a complex urban environment like Fairbanks. Note that Fairbanks is surrounded by hills to three sides.

4.2 Suggested Future Research

The WRF-CMAQ simulations performed for this study were made with the draft version of Fairbanks emission inventory of 2008 prepared by Sierra Research Inc.. This emission inventory was the only bottom-up emission inventory available at the time of the start of the project. Meanwhile Sierra Research Inc. updated their emission inventory twice for Fairbanks. Simulation with the Alaska adapted WRF-CMAQ with this updated emission inventory would potentially archive better performance of WRF-CMAQ and potentially higher accuracy in interpolated concentrations. Thus, we recommend that WRF-CMAQ simulations with the updated inventory should be made and replace the current WRF-CMAQ simulation results that serve as data base for the interpolation algorithm.

Wildfires may lead to extremely unhealthy concentrations in summer [*Mölders and Kramm*, 2007]. Thus, the FNSB may desire to perform drives during these times for public advisory. The current interpolation algorithms were developed based on simulations for episodes in deep winter when calm wind and extremely low temperatures are common. These conditions were identified by *Tran and Mölders* [2011] as typical candidates for exceedances of the NAAQS at the State Office Building site. The efficiency of the interpolation algorithms in interpolating $PM_{2.5}$-concentrations under conditions with stronger winds and/or higher temperatures (e.g., for October, March, summer) was beyond the scope of this project, but seems worth to be examined in the future. Expanding the database for such situations would require creating some WRF-CMAQ datasets.

REFERENCES

Barnard, J., Fast, J., Paredes-Miranda, G., Arnott, W., Laskin, A., 2010. Technical Note: Evaluation of the WRF-Chem 'aerosol chemical to aerosol optical properties' module using data from the MILAGRO campaign. *Atmospheric Chemistry and Physics* 10, pp. 7325-7340.

Boylan, J.W., Russell, A.G., 2006. PM and Light Extinction Model Performance Metrics, Goals, and Criteria for Three-Dimensional Air Quality Models. *Atmospheric Environment* 40, pp. 4946-4959

Cahill, C.F., 2003. Asian aerosol transport to Alaska during ACE-Asia. *Journal Geophysical Research* 108, 8664.10.1029/2002jd003271.

Chou, M.-D., Suarez, M.J., 1994. An efficient thermal infrared radiation parameterization for use in general circulation models. *NASA Tech. Memo* 104606, 3, 85pp.

Gaudet, B.J., Stauffer, D.R., 2010. *Stable Boundary Layers Representation in Meteorological Models in Extremely Cold Wintertime Conditions*. pp. 60.

Grell, G.A., Dévényi, D., 2002. A generalized approach to parameterizing convection combining ensemble and data assimilation techniques. *Geophys. Res. Lett.* 29, 1693, doi:10.1029/2002GL015311.

Houyoux, M.R., Vukovich, J.M., Brandmeyer, J., 2007. SMOKE User Manual, version 2.3. MCNC Environmental Programs, Research Triangle Park: NC, USA.

Hong, S.-Y., Lim, J.-O.J., 2006. The WRF Single-Moment 6-class microphysics scheme (WSM6). *Journal Korean Meteorological Society* 42, 129-151.

Janjić, Z.I., 1994. The step-mountain eta coordinate model: further developments of the convection, viscous sublayer and turbulence closure schemes. *Mon. Wea. Rev.* 122, 927-945.

Leelasakultum, K., Mölders, N., Tran, H.N.Q., Grell, G.A., 2012. Potential impacts of the introduction of low sulfur fuel on $PM_{2.5}$-concentrations at breathing level in a subarctic city. *Advances in Meteorology*.

Mlawer, E.J., Taubman, S.J., Brown, P.D., Iacono, M.J., Clough, S.A., 1997. Radiative transfer for inhomogeneous atmospheres: RRTM, a validated correlated-k model for the longwave. *J. Geophys. Res.* 102(D14), 16663-16682, doi:16610.11029/16697JD00237.

Mölders, N., Kramm, G., 2007. Influence of wildfire induced land-cover changes on clouds and precipitation in Interior Alaska – A case study. *Atmos. Res.*, 84, 142-168.

Mölders, N., 2008. Suitability of the Weather Research and Forecasting (WRF) model to predict the June 2005 fire weather for Interior Alaska, *Wea. Forecast.*, *23*, 953-973.

Mölders, N., Kramm, G., 2010. A case study on wintertime inversions in Interior Alaska with WRF. *Atmos. Res.* 95: 314-332.

Mölders, N., 2010. Comparison of Canadian Forest Fire Danger Rating System and National Fire Danger Rating System fire indices derived from Weather Research and

Forecasting (WRF) model data for the June 2005 Interior Alaska wildfires, *Atmospheric Research*, *95*(2-3), 290-306.

Mölders, N., Tran, H. N. Q., Quinn, P., Sassen, K. , Shaw, G. E., and Kramm, G., 2011a. Assessment of WRF/Chem to capture sub-Arctic boundary layer characteristics during low solar irradiation using radiosonde, SODAR, and station data, *Atmospheric Pollution Research*, *2*, 283-299.

Mölders, N., Tran, H.N.Q, Leelasakultum, K., 2011b. Investigation of means for $PM_{2.5}$ mitigation through atmospheric modeling. Final report, 12/1/08 – 12/31/10, 75pp.

Mölders, N., Leelasakultum, K., 2011. CMAQ Modeling: Final Report Phase I. *Rep.*, 62 p.

Mölders, N., Tran, H.N.Q., Cahill, C.F., Leelasakultum, K., Tran, T.T., 2012. Assessment of WRF/Chem $PM_{2.5}$-forecasts using mobile and fixed location data from the Fairbanks, Alaska winter 2008/09 field campaign. *Atmos. Poll. Res.*, 3, 180-191.

Operation Guidance for the Community Multiscale Air Quality (CMAQ) Modeling System Version 4.7.1., 2010, Community Modeling and Analysis System Institute for the Environment University of North Carolina at Chapel Hill, NC 27599.

Peckham, S.E., Fast, J.D., Schmitz, R., Grell, G.A., Gustafson, W.I., McKeen, S.A., Ghan, S.J., Zaveri, R., Easter, R.C., Barnard, J., Chapman, E., Salzmann, M., Wiedinmyer, C., Freitas, S.R., 2009. *WRF/Chem Version 3.1 User's Guide*. pp.78.

Tran, H.Q.N, Mölders, N., 2011. Investigations on meteorological conditions for elevated $PM_{2.5}$ in Fairbanks, Alaska, *Atmos. Res.*, 99, 39-49.

Tran, T.T, Newby, G., Mölders, N., 2011. Impacts of emission changes on sulfate aerosols in Alaska, *Atmos. Environ.*, 45, 3078-3090.

Smirnova, T.G., Brown, J.M., Benjamin, S.G., Kim, D., 2000. Parameterization of cold season processes in the MAPS land-surface scheme. *J. Geophys. Res.* 105(D3), 4077-4086, doi:4010.1029/1999JD901047.

von Storch, H., Zwiers, F.W., 1999. Statistical Analysis in Climate Research,Cambridge University Press, 484pp.

Yarker, M. B., PaiMazumder, D. , Cahill, C. F., Dehn, J., Prakash, A., and Mölders, N., 2010. Theoretical investigations on potential impacts of high-latitude volcanic emissions of heat, aerosols and water vapor and their interactions on clouds and precipitation, *The Open Atmospheric Science Journal*, *4*, 24-44.

Zhao, Z., Chen, S.-H., Kleeman, M.J., Tyree, M., Cayan, D., 2011. The Impact of Climate Change on Air Quality–Related Meteorological Conditions in California. Part I: Present Time Simulation Analysis. *Journal Climate,* 24, 3344-3361.

APPENDICES
Appendix A
Paper published:
Mölders, N., Tran, H.N.Q., Cahill, C.F., Leelasakultum, K., Tran, T.T., 2012. Assessment of WRF/Chem $PM_{2.5}$-forecasts using mobile and fixed location data from the Fairbanks, Alaska winter 2008/09 field campaign. *Atmos. Poll. Res*. doi: 10.5094/APR.2012.018.
Downloadable at: http://www.atmospolres.com/articles/Volume3/issue2/APR-12-020.pdf

Appendix B

Example of a File that Contains Mobile Measurement Data to be Used in the Interpolation Algorithm

<File name: 2011006.csv>

#Date,hour,minute,second,Latitude,Longitude,Elevation,Temperature,PM2.5_MASS

2011006,13,53,36,64.81915715,-147.77797032,125.1087646,-8.15,1.5

2011006,13,53,38,64.81915732,-147.77796948,125.1087646,-7.9,5.8

2011006,13,53,40,64.81915715,-147.77796990,125.1087646,-7.84,4.8

2011006,13,53,42,64.81915724,-147.77797032,125.1087646,-8.08,6

2011006,13,53,44,64.81915698,-147.77797099,125.1087646,-8.02,7.6

2011006,13,53,46,64.81915673,-147.77797082,125.1087646,-8.08,7.4

2011006,13,53,48,64.81915665,-147.77797066,125.5893555,-8.21,7.4

2011006,13,53,50,64.81915665,-147.77797108,125.5893555,-8.02,7.1

2011006,13,53,52,64.81915656,-147.77797217,125.1087646,-8.21,7.6

2011006,13,53,54,64.81915690,-147.77797292,125.1087646,-8.4,7.9

2011006,13,53,56,64.81915740,-147.77797351,125.1087646,-8.02,7.5

2011006,13,53,58,64.81915791,-147.77797367,125.5893555,-8.27,6.3

2011006,13,54,0,64.81915866,-147.77797326,125.5893555,-7.9,6.6

2011006,13,54,2,64.81915925,-147.77797258,125.1087646,-7.9,6.2

2011006,13,54,4,64.81915983,-147.77797191,125.5893555,-8.15,7.7

2011006,13,54,6,64.81916042,-147.77797158,125.5893555,-7.97,8.5

2011006,13,54,8,64.81916059,-147.77797158,125.5893555,-8.08,10.7

2011006,13,54,10,64.81916059,-147.77797149,-999,-999,-999

Appendix C

Example of the Application of the Interpolation Algorithm to a Region in Southeast Alaska

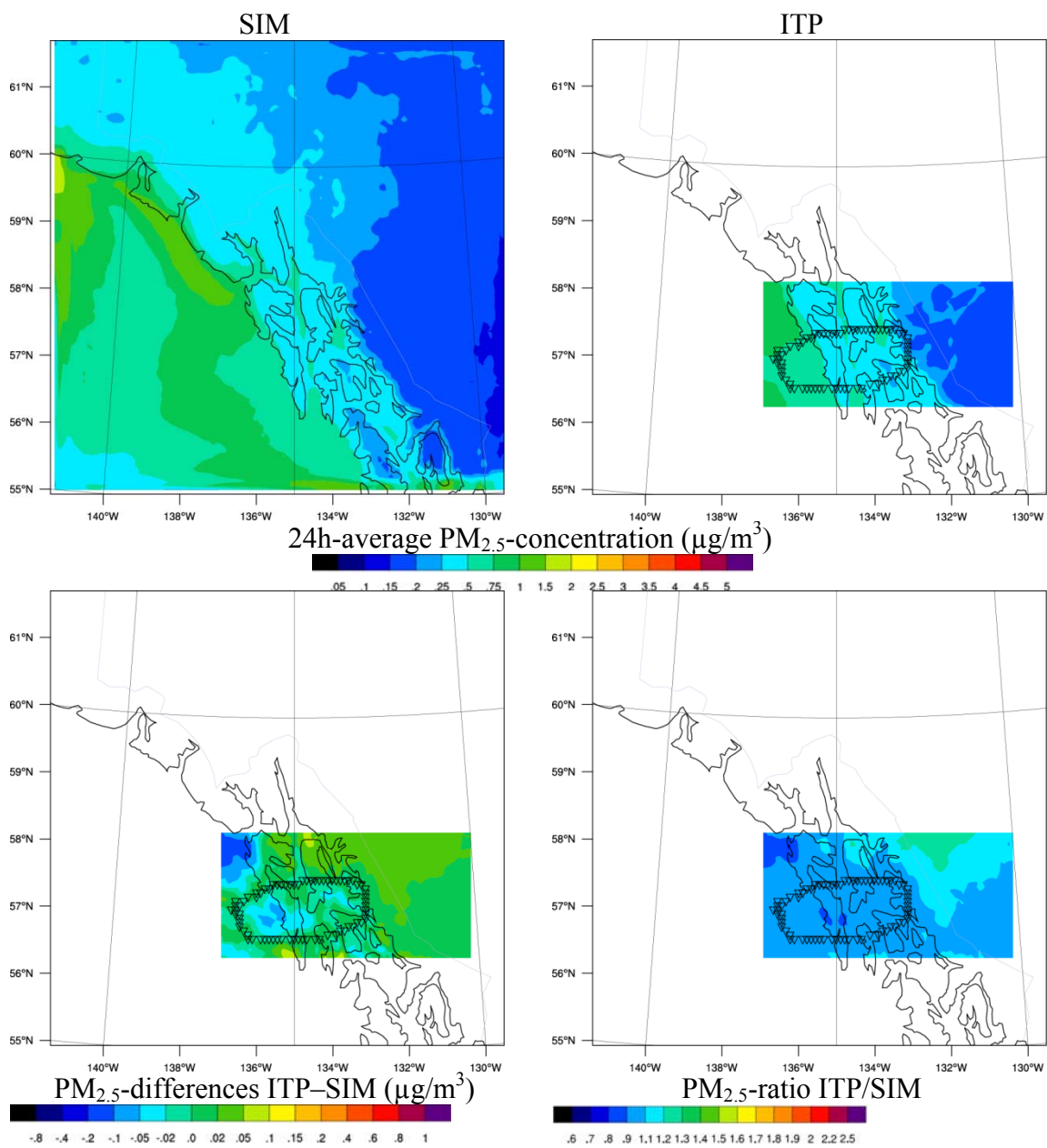Here the transferability of the developed interpolation algorithm is demonstrated.

Fig. C1. Interpolated (ITP) vs. simulated, i.e. "grand truth" (SIM) $PM_{2.5}$-concentrations as obtained with the developed interpolation algorithm using the WRF/Chem-data from *Mölders and Daengngern* [2012; pers. comm.] as "proxy" for observation in Southeast Alaska. The black triangle indicates the grid-cells of the assumed sniffer route on this day. Here a sniffer is assumed that goes on a ferry sometimes.

To demonstrate the transferability of the interpolation algorithm we used WRF/Chem $PM_{2.5}$-concentration data from a study performed by *Mölders and Daengngern* [2012; pers. comm.].

We used WRF/Chem data they obtained for June of their study to create a data base for the interpolation algorithm. We used another simulation of their study again as "grand truth" as we had no mobile measurements for that region. We assumed an arbitrary route, pulled the $PM_{2.5}$-concentrations along the assumed route as "proxy" for measurements. We applied the interpolation algorithm and compared the interpolated with the WRF/Chem simulated $PM_{2.5}$-concentrations (Fig. C1).